

Systematics of the genus *Hormiops* Fage, 1933 (Hormuridae, Scorpiones)

Lionel Monod

Département des arthropodes et d'entomologie I, Muséum d'histoire naturelle, Route de Malagnou 1, CH-1208 Genève, Switzerland. E-mail: lionel.monod@ville-ge.ch

Abstract: Based on a recently published phylogeny of Australasian hormurid scorpions, *Hormiops* Fage, 1933, previously considered a doubtful taxon by some authors, is now reinstated as a valid genus. These lithophilous scorpions are currently only recorded from two groups of granitic islands in the South China Sea, the Côn Đảo Archipelago near the southern tip of Vietnam and the Seribuat Archipelago off the south-east coast of Peninsular Malaysia. Each of these archipelagos is harbouring a distinct species. Newly collected specimens enable the examination of unknown or inadequately studied morphological characters, such as cuticle ornamentation, hemispermatophores and book lungs. Based on these new data, updated descriptions with high resolution illustrations of important diagnostic characters are provided for *H. davidovi* Fage, 1933 and *H. infulcra* Monod, 2014.

Keywords: *Hormiops davidovi* - *H. infulcra* - taxonomy - South China Sea - Vietnam - Malaysia - lithophilous.

INTRODUCTION

The validity of the hormurid genus *Hormiops*, described from the Vietnamese Côn Sơn Island, formerly known as Poulo Condore and part of the Côn Đảo Archipelago, was confirmed only recently (Monod & Prendini, 2015). *Hormiops* Fage, 1933 was previously considered as a junior synonym of *Liocheles* Sundevall, 1833 by Lourenço (1989), Fet (2000) and Prendini (2000). Fet (2000) placed *Hormiops davidovi* Fage, 1933 in the synonymy of *Liocheles australasiae* (Fabricius, 1775), whereas Prendini (2000) recognized it as a valid species within *Liocheles*. Lourenço & Monod (1999) reinstated the genus, but their decision was not accepted by Prendini (2000) who deemed the diagnostic characters insufficient for a generic distinction. Monod & Prendini (2015) confirmed the validity of the genus *Hormiops* based on a proper phylogenetic framework. A second species, *H. infulcra*, discovered on granitic islands off southern Peninsular Malaysia was subsequently added to the genus (Monod, 2014). Two species of *Hormiops* are thus currently recognized: *Hormiops davidovi* from the Côn Đảo Archipelago near the southern tip of Vietnam, and *H. infulcra* from the Seribuat Archipelago off the south-eastern coast of Peninsular Malaysia. Field surveys were recently conducted in both archipelagos and these yielded sufficiently large series of specimens. Thus far the limited material available and the poor state of preservation of *H. davidovi* types (faded colouration and loss of cuticle fluorescence) had prevented a complete and accurate study of characters such as cuticle

ornamentation, hemispermatophores and book lungs. The newly collected material enabled the examination of these characters, which were previously unknown or inadequately studied, and allowed updated descriptions with high quality illustrations of important diagnostic character for both species.

The present contribution was originally part of a manuscript on the systematics and biogeography of the genus *Hormiops*. The taxonomic section was greatly reduced at the editor's request in order to fit the standard of the journal, and thus a shorter manuscript, which only includes diagnoses and illustrations of the most important characters for both *Hormiops* species, was published (Monod, 2014). The extensive descriptions and illustrations that could not be incorporated in this first paper are presented here.

MATERIAL AND METHODS

Fieldwork: Scorpions were collected during the day by inspecting rock crevices and exfoliations, and at night with ultraviolet (UV) light (Stahnke, 1972) using a portable Maglite lamp equipped with a UV led retrofit (Xenopus electronix, Austin, TX, U.S.A.).

Georeferencing: Exact geographical coordinates of collecting localities were recorded using a portable GPS device (Garmin E-trek Summit). Only coarse data, rounded to the nearest 10 seconds, are provided in the present publication following the recommendations of

Chapman & Grafton (2008). Geographical coordinates for records without GPS data were traced by reference to gazetteers and the Geonet Names server (<http://earth-info.nga.mil/gns/html/index.html>) and are given between brackets.

Abbreviations: Depositories containing material examined in the present study are abbreviated as follows: LKCM, Lee Kong Chian Natural History Museum, National University of Singapore (Singapore), MHNG, Muséum d'histoire naturelle (Geneva, Switzerland); MNHN, Muséum National d'Histoire Naturelle (Paris, France). Other abbreviations: NP, National park.

Examination and dissection: Specimens were examined with a Zeiss Stemi SV8 stereomicroscope. Hemispermatothores were dissected from adult male specimens using microsurgical scissors and forceps immediately after the animals were euthanized. Paraxial organ tissue was then removed manually with forceps. Dissecting the specimens as early as possible ensure that paraxial organ tissue has not stiffened yet and can be removed more easily without damaging the hemispermatothores. This is particularly recommended for small, weakly sclerotized hemispermatothores like those of *Hormiops*.

Morphological terminology and mensuration: Morphological terminology follows Vachon (1956, 1963) for cheliceral dentition, Stahnke (1970) for pedipalp segmentation, Vachon (1974) for trichobothrial patterns, Couzijn (1976) for leg segmentation, Lamoral (1979) and Monod & Volschenk (2004) for hemispermatothore, Kamenz *et al.* (2005) and Kamenz & Prendini (2008) for book lungs, and Prendini (2000) for carapace sulci and sutures, and pedipalp and metasomal carinae. Measurements follow Stahnke (1970) and were recorded in mm using an ocular micrometer or digital calipers.

Photographs and illustrations: High resolution fluorescence images of diagnostic characters were taken under long-wave UV (Volschenk, 2002, 2005) and visible light with a custom-built stacking system at the MHNG. Zerene Stacker (Zerene Systems, Richland, WA, U.S.A.) was used to fuse images taken at different focal planes into a single image with greater depth of field. Line drawings of hemispermatothores were produced using a camera lucida mounted on the stereomicroscope. Pencil sketches were subsequently inked and scanned for further processing and editing. Illustrations and photographs were edited (background removal and contrast adjustment) in Adobe Photoshop CS5, and plates prepared with Adobe Illustrator CS5 (both from Adobe systems, San Jose, CA, U.S.A.). Colour drawings were produced as digital media based on scientific illustrations and photographs of live specimens to accurately illustrate the colours present in life.

Scanning electron microscopy (SEM): SEM was used to explore the fine structures of post-insemination spermatophores and book-lungs. Spermatophores were obtained by placing male and female scorpions in a terrarium. When mating occurred, spermatophores were retrieved from the enclosures and placed in 75% ethanol immediately after copulation. They were then dehydrated in a graded alcohol series, critical point dried in a SPI-DRY critical point dryer (SPI supplies, West Chester, PA, U.S.A.), mounted on standard aluminium stubs (diameter 12.5 mm, height 6 mm; Agar Scientific, Essex, U.K.), and finally sputter-coated with gold in a Cressington Sputtercoater 108 Auto. Half of one sternite was dissected from specimens preserved in 100% ethanol. Sternites and book lungs were sliced transversally at the spiracle level, leaving an anterior part bearing the lungs per se and a posterior part bearing the atrial wall and posterior spiracle edge. Alcohol was removed from these two parts by critical point drying. The anterior part was then sliced sagittally to expose lamella surfaces. The dissected structures were then mounted on common stubs and sputter-coated with gold. Samples were examined with a Zeiss DSM940A SEM.

Mapping: Distribution maps were produced using ArcGIS version 9.3 (Environmental Systems Research Institute, Redlands, CA, U.S.A.) by superimposing locality record coordinates on a SRTM 90 m (3 arc-second) digital elevation model (Jarvis *et al.*, 2008) and on a SRTM 1 km (30 arc-second) global bathymetry dataset (Becker *et al.*, 2009).

Allometry: The pronounced sexual dimorphism of pedipalps observed in the two *Hormiops* species was analysed by comparing allometric slopes of a standardized major axis (SMA; Kermack & Haldane, 1950) of males and females. The degree of allometry is traditionally measured by the equation $Y = aX^\alpha$, where X is the measurement of a basic, independent character such as body length, Y the measurement of a dependent character such as pedipalp size whose allometric index α is to be determined, and a is a normalization constant also known as the 'Y intercept' or elevation of the slope. The actual computation usually proceeds through a regression analysis using the linear analogue of the allometric equation ($\log Y = \alpha \log X + \log a$). SMA analyses were used to determine the lines-of-best-fit for each bivariate group. SMA regression is methodologically more appropriate to assess allometric relationships between two variables than ordinary least-square (OLS) regression (Ricker, 1984; Green, 1992; Warton *et al.*, 2006; Bonduriansky, 2007; Claude, 2008). OLS regression estimates the line of best fit by minimizing the sum of squares of residuals measured in the Y direction. It basically attributes all residual variation to Y, which translates into an underestimation of the allometric slope. On the other hand, SMA

regression assumes equal error in both measurements, X and Y, and thus provides a more accurate estimate of the axis.

Length of pedipalp chela, patella, femur and of carapace of mature specimens of *H. davidovi* (11 males and 22 females) and *H. infulcra* (25 males and 25 females) were measured. Pedipalp length was calculated by adding up chela, patella and femur lengths, and the carapace was used as a measure of overall body length. Analyses of allometric relationships between pedipalp and body sizes were implemented with the "SMATR" module version 3.2.3 (Warton *et al.*, 2011; Warton *et al.*, 2012) for the R statistical package version 2.12.2 (R Development core Team, 2011). Bivariate scatter plots of the pedipalp size (Y) versus body size (X) with fitted SMA slopes for males and females were computed for each species. Each slope was tested for allometry using the *slope.test* command that estimates whether the residual axis and fitted axis scores are uncorrelated under a hypothetical allometric slope α (Warton *et al.*, 2006). Here, the α value was set at 1.0 in order to assess significant deviation from isometry (*Ho*). Intersexual differences in allometric slope were then estimated for each species using the likelihood

ratio test proposed by Flury (1984) and Warton & Weber (2002). Significance levels for all tests were set at $P=0.05$.

SYSTEMATICS

Family Hormuridae Laurie, 1896

Genus *Hormiops* Fage, 1933

Hormiops davidovi Fage, 1933

Figs 1A-C, 2-12, 13A, 14, 15, Tab. 1

Hormiops davidovi Fage, 1933: 32-33, figs 1, 2, pl. I, figs a-c. – Fage, 1936: 181. – Kästner, 1941: 234, fig. 215. – Takashima, 1945: 94, 95. – Fage, 1946: 71. – Vachon, 1974: fig. 80. – Kovařík, 1998: 132. – Lourenço & Monod, 1999: 343-344, figs 1-4. – Lourenço, 2011: 774. – Monod, 2014: 601-602, figs 1a, c, 2a, 3a-b, d, f-g.

Hormiops davidovi. – Monod & Prendini, 2015: 5-16, 24-25, 34, fig. 1A.[misspelling].

Liocheles australasiae. – Fet, 2000: 395.

Liocheles davidovi. – Prendini, 2000: 72. – Monod & Volschenk, 2004: 686.



Fig. 1. Live specimens of the species in the hormurid genus *Hormiops* Fage, 1933. (A, C) *Hormiops davidovi* Fage, 1933, male (A) and female (C). (B, D) *Hormiops infulcra* Monod, 2014, male (B) and female (D).



Fig. 2. *Hormiops davidovi* Fage, 1933, habitus of male, dorsal aspect, reconstruction based on scientific illustrations and photographs of live specimens. Scale, 5 mm.



Fig. 3. *Hormiops davidovi* Fage, 1933, habitus, dorsal (A-B) and ventral (C-D) aspects. (A, C) Male (MHNG, sample VMI-12/04). (B, D) Female (MHNG, sample VMI-12/04). Scale, 5 mm.

Material: *Types:* MNHN-RS 0562; male lectotype, 1 female and 1 juv. paralectotypes; Vietnam, Poulo Condore [=Côn Sơn Island, N8°42'00" E106°36'00"], S off the coast of Vietnam; in forest, under stones; II.1930/IV.1931; M. C. Dawydoff. – *Other material:* MNHN-RS 0499; 1 female, 11 juv.; Vietnam, Poulo Condore Island [=Côn Sơn Island, N8°42'00" E106°36'00"]; M. Germain. – MHNG; 1 male, 3 females; sample VMI-12/01, Côn Đảo NP, Côn Sơn Island, trail to Ong Dung Beach; rainforest, in rock crevices (granitic boulders); 8.I.2012; leg. L. Monod. – MHNG; 4 males, 4 females, 20 juv.; sample VMI-12/02, Côn Đảo NP, Côn Sơn Island, trail to Soy Ray plantation, N8°41' E106°35'; 50-180 m, rainforest, in rock crevices; 9.I.2012; leg. L. Monod. – MHNG; 2 males, 4 females; sample VMI-12/04, Côn Đảo NP, Côn Sơn Island, trail to Dat Tham Beach, N8°42' E106°35'; 150 m, rainforest, in rock crevices; 10.I.2012; leg. L. Monod. – MHNG; 1 male, 5 females, 2 juv.; sample VMI-12/07, Côn Đảo NP, Côn Sơn Island, trail to Dam Tre Bay, N8°44' E106°39'; 15-70 m, rainforest, in rock crevices; 11.I.2012; leg. L. Monod. – MHNG; 1 female; sample VMI-12/10, Côn Đảo NP, Ba Island, N8°38' E106°33'; rainforest, in rock crevices; 12.I.2012; 60 m, leg. L. Monod.

Description of adult male: *Coloration:* Dorsal surface of chelicera manus orange-brown, with darker infuscation; fingers dark brown to black (Figs 1A, 2). Carapace and tergites dark brown to black. Pedipalps reddish brown, with darker infuscation; carinae and fingers black. Legs yellow to orange, prolateral carina of femora black, femora and patellae II-IV with darker infuscation. Coxapophyses I-II and sternites orange to dark brown; eoxapophyses III-IV, sternum, genital operculum and pectines yellowish to orange-brown. Metasoma dark brown to black. Telson yellow, aculeus reddish black.

Cuticle: Non-granular surfaces of carapace, pedipalps, legs, mesosoma and metasoma finely punctated.

Carapace: Anterior margin with shallow median notch (Fig. 4A). Anterior furcated sutures vestigial. Median ocular tubercle situated anteromedially, very low, small, occupying about one ninth of carapace width at that point; superciliary carinae absent; median ocelli present, at least twice the size of lateral ocelli, separated by at least half diameter of median ocellus. Two pairs of lateral ocelli equal in size, equidistant and adjacent to one another. Postocular carapace margin without spines or tubercles. Surfaces finely and densely granular (creating a matte appearance) except anteriorly; anterolateral surfaces and frontal lobes smooth, fine granulation restricted to surface adjacent to median longitudinal sulcus (Fig. 4A, C).

Chelicerae: Median and basal teeth of fixed finger fused into a bicuspid. Dorsal margin of movable finger with four teeth (one subdistal and one basal); dorso-distal tooth smaller than ventro-distal tooth; ventral margin smooth.

Pedipalps: Pedipalp segments long and slender (Figs 1A, 2, 3A, C, 5B-E, G-J, L-O), with femur length approximately 1.5 times carapace length (Tab. 1). Chela almost aetose.

Chela fingers: Dentate margins of fixed and movable fingers linear (without lobe and notch) distally, with two rows of primary denticles of similar size, these rows merged to each other basally, accessory denticles absent (Fig. 6A-B). Fixed finger: basal lobe weakly developed; suprabasal notch well developed (Figs 6A-B, 7A). Movable finger: basal lobe absent; suprabasal lobe well developed, wider than high, gently rounded dorsally, not overlapping fixed finger; suprabasal lobe and corresponding suprabasal notch on fixed finger contiguous, no proximal gap or at most a reduced gap evident when fingers closed.

Pedipalp carinae: Femur (Fig. 5L-O): internomedian ventral carina vestigial, comprising two large spiniform granules situated proximally and medially on segment; internomedian dorsal carina vestigial, comprising a single basal spine; dorsointernal carina with coarse spiniform granules, more strongly developed than dorsoexternal carina; dorsoexternal carina developed as a band of granules in proximal half and as an almost smooth ridge in distal half; ventroexternal carina with coarse spiniform granules; ventromedian carina obsolete, granular proximally; ventrointernal carina with coarse spiniform granules. Patella (Fig. 5G-J): prolateral dorsal and prolateral ventral spiniform processes equally developed and fused medially, forming a prominent median spine, angled approximately 45° relative to longitudinal axis of segment; internodorsal carina with coarse spiniform granules; dorsointernal carinae developed as a band of granules proximally, and as a smooth ridge medially; dorsoexternal carina distinct, developed as a faint costate ridge; externomedian carina granular; ventroexternal carina distinct, developed as a smooth or faintly eostate ridge; ventrointernal carina with coarse spiniform granules. Chela manus (Fig. 5B-E): dorsal secondary carina obsolete; digital carina distinct, costate to granular, more strongly developed than external secondary carinae; external secondary carinae weakly developed, granular; ventroexternal carina costate; ventromedian and ventrointernal carinae obsolete; internomedian carina distinct, granular.

Pedipalp chela maerosculpture: Femur (Fig. 5L-O): dorsal intercarinal surface smooth, fine granulation limited to proximal and retrolateral edges; retrolateral intercarinal surface smooth, sparsely granular ventrally; ventral intercarinal surface granular proximally, distal half smooth; prolateral intercarinal surface finely granular. Patella (Fig. 5G-J): dorsal intercarinal surface smooth, with prolateral edge and proximal end sparsely granular; retrolateral intercarinal surface smooth; ventral intercarinal surface smooth, with prolateral edge faintly granular; prolateral intercarinal surface finely granular, with distal extremity smooth. Chela manus (Fig. 5B-E): dorsal intercarinal surface with scattered granules fused into a reticulated network, becoming denser on prolateral and

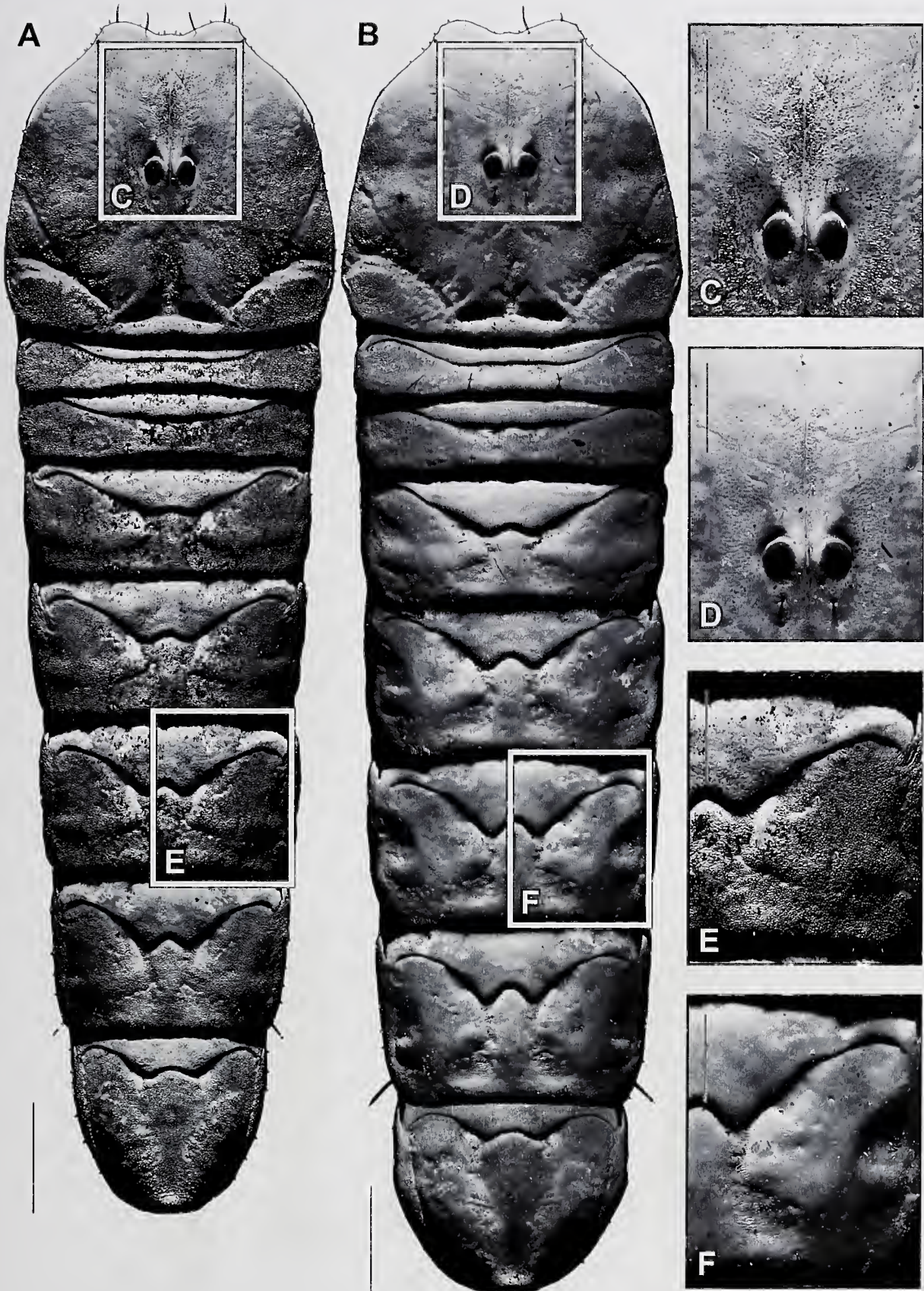


Fig. 4. *Hormiops davidovi* Fage, 1933, carapace and mesosomal tergites, illustrating ornamentation and macrosulpture of cuticle (A-B), with detailed view of carapace (C-D) and of tergite V (E-F), dorsal aspect. (A, C, E) Male (MHNG, sample VMI-12/04). (B, D, F) Female (MHNG, sample VMI-12/04). Scale, 2 mm (A, B), 1 mm (C-F).

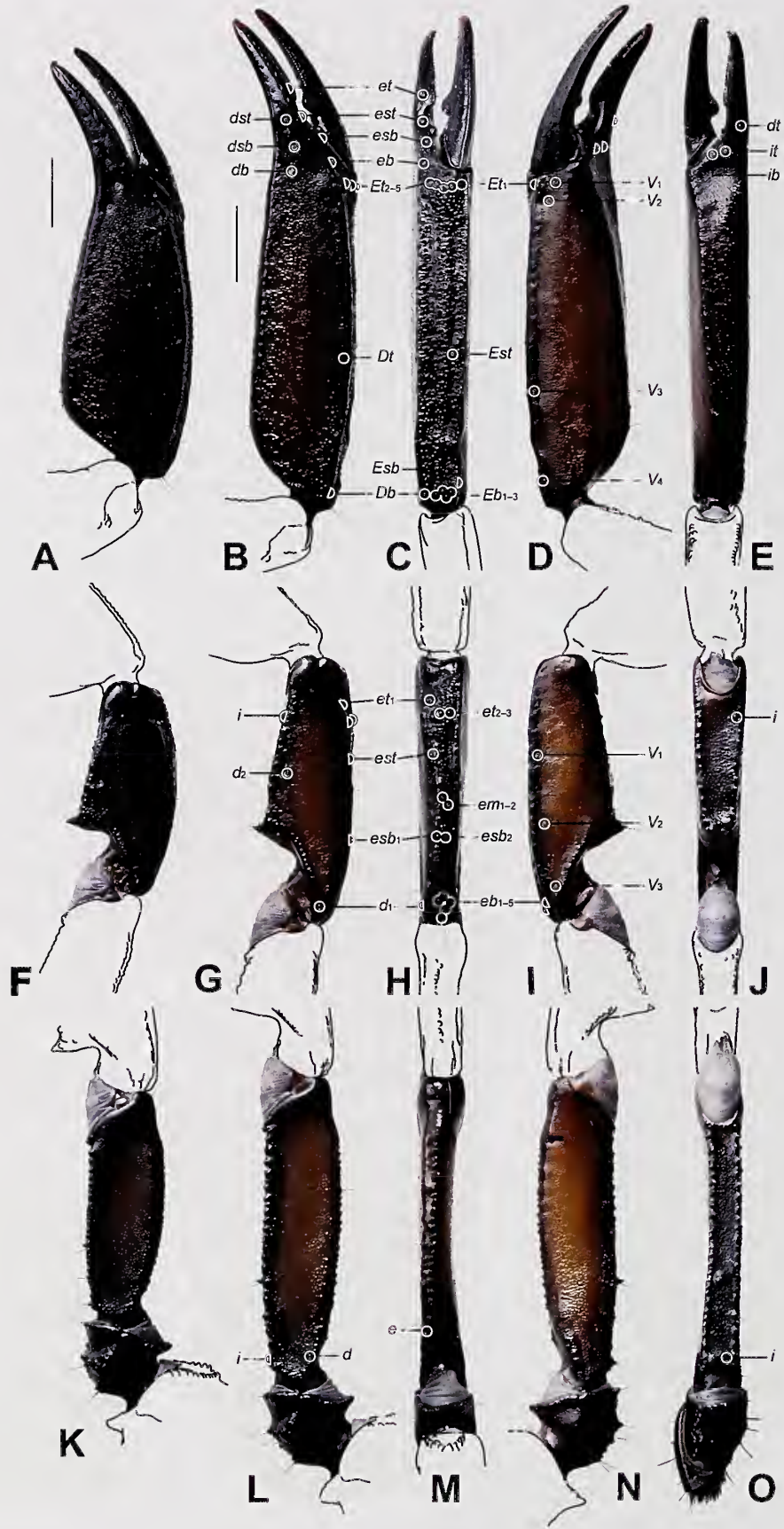


Fig. 5. *Hormiops davidovi* Fage, 1933, pedipalp chela (A-E), patella (F-J), femur and trochanter (K-O), dorsal (A, B, F, G, K, L), retrolateral (C, H, M), ventral (D, I, N) and prolateral (E, J, O) aspects showing trichobothrial pattern. (A, F, K) Female (MHNG, sample VMI-12/04). (B-E, G-J, L-O) Male (MHNG, sample VMI-12/04). Scales, 2 mm.

Table 1. *Hormiops davidovi* Fage, 1933, measurements (in mm) of adult males and females.

Status	Lectotype				Paralectotype			
	male	male	male	male	female	male	female	female
Sex								
Repository	MNHN	MHNG	MHNG	MHNG	MNHN	MHNG	MHNG	MHNG
Registration/sample	RS 0562	VM-12/02	VM-12/02	VM-12/04	RS 0562	VM-12/01	VM-12/04	VM-12/04
Total length	30	32	35	37	37	32	37	34
Carapace length	4.6	4.5	5.5	5.5	5.1	4.9	5.7	5.2
Carapace anterior width	2.2	2.5	2.7	2.8	2.5	2.4	2.8	2.8
Carapace posterior width	4.6	5	5.9	6.1	5.5	5	6.3	5.7
Femur length	6.2	6.6	8.9	8.5	6.1	5.6	6.6	6.1
Femur width	1.8	2.1	2.3	2.3	2.1	2.1	2.3	2.1
Patella length	5.4	6	7.8	7.4	5.7	5.3	5.9	5.6
Patella width	2.1	2.4	2.9	2.5	2.4	2.5	2.8	2.5
Chela length	10.2	11.4	14.3	13.9	10.9	10.2	12.2	11.2
Chela manus width	2.5	2.5	2.9	2.9	3.2	3	3.8	3.1
Chela manus height	1.5	1.5	1.8	1.7	1.8	1.5	1.7	1.6
Chela movable finger length	4	4.4	5.3	5.3	4.2	4.5	5.4	5.1
Metasomal segment I length	1.6	1.5	1.9	1.9	1.7	1.5	2.1	1.6
Metasomal segment I width	1.2	1.2	1.4	1.3	1.2	1.2	1.4	1.2
Metasomal segment V length	2.2	2.5	2.9	2.9	2.5	2.3	2.8	2.4
Metasomal segment V width	0.7	0.7	0.8	0.8	0.8	0.8	0.8	0.8
Metasomal segment V height	0.9	1	1.1	1.1	1.1	1	1.1	1
Telson vesicle width	0.7	0.8	0.9	0.8	0.8	0.8	0.8	0.8
Telson vesicle height	0.7	0.8	0.9	0.9	0.8	0.8	0.9	0.8

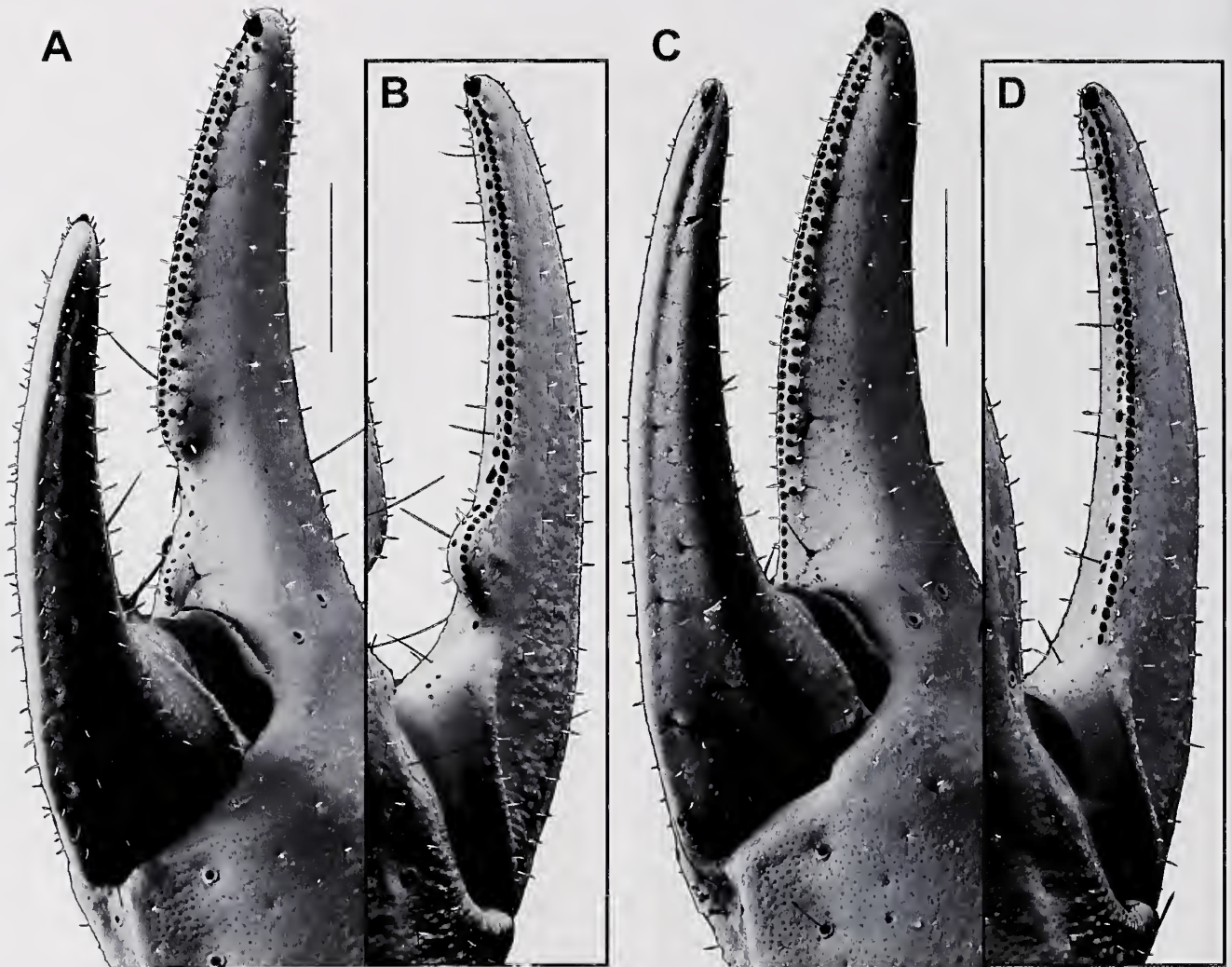


Fig. 6. *Hormiops davidovi* Fage, 1933, pedipalp chela, dentate margins of fixed (A, C) and movable (B, D) fingers. (A-B) Male (MHNG, sample VMI-12/04). (C-D) Female (MHNG, sample VMI-12/04). Scale, 1 mm.

retrolateral edges; retrolateral intercarinal surface granular; ventral intercarinal surface smooth, with retrolateral edge faintly granular; prolateral intercarinal surface sparsely granular. Chela fingers smooth; surface around *db*, *dsb* and *dst* trichobothria of fixed finger smooth.

Trichobothria: Pedipalp orthobothriotaxic, accessory trichobothria absent (Fig. 5B-E, G-J, L-O). Patella: *d*₂ trichobothria distal to patellar process; five *eb* trichobothria arranged in two groups *eb*_{1,2} and *eb*_{2,3}; two *esb* trichobothria; two *em* trichobothria; one *est* trichobothrium; three *et* trichobothria; three *V* trichobothria. Chela manus with *Dt* situated slightly proximal to midpoint; *Eb*₃ situated close to *Eb*_{1,2}; *Esb* basal, aligned with *Eb* series; *Est* situated at or near midpoint; four *V* trichobothria, with *V*₃ and *V*₄ separated. Fixed chela finger with *db* situated on dorsal surface; *esb*, *eb*, *est* and *et* equidistant (distance *est-esb* similar to distance *esb-eb*); *eb* situated at base of finger, proximal to point of articulation between fixed and movable fingers, above *esb-et* axis;

esb situated at base of finger, proximal to point of articulation between fixed and movable fingers, below *est-et* axis; two *i* trichobothria proximal to base of fixed finger. *Coxosternal region*: Leg III coxae without swelling or bulge anterodistally. Sternum equilateral pentagonal (Fig. 8A); anterior width slightly exceeding posterior width; length exceeding posterior width.

Legs: Femora I-IV with ventral surfaces bearinate, proventral and retroventral carinae granular. Retroventral margins of tibiae I and II without setiform macrosetae. Pro- and retroventral margins of basitarsi I-IV with 4 spiniform macrosetae. Telotarsi I-IV: pro/retroventral margins each with 4/5, 4/5, 4/5 and 5/5 setiform macrosetae (Fig. 9D-E); ventromedian row of spinules absent; dorsomedian lobe pronounced; laterodistal lobes truncate; unguis curved, shorter than telotarsus.

Genital operculum composed of two subtriangular sclerites (Fig. 8A).

Pectines: Moderately elongated, distal edge reaching but

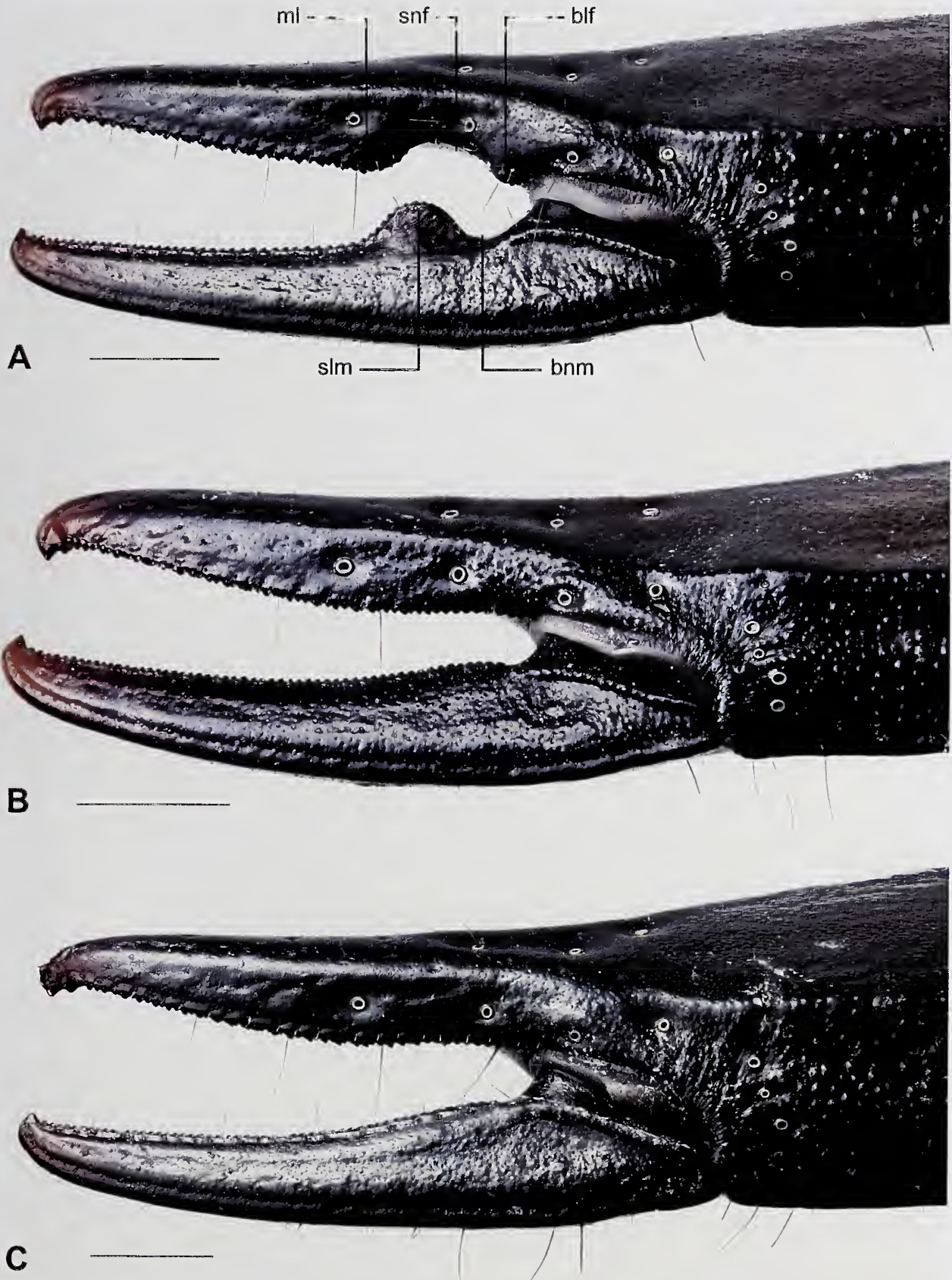


Fig. 7. *Hormiops davidovi* Fage, 1933, pedipalp chela, retrolateral aspect showing dentate margin of chela fingers. (A) Male (MHNG, sample VMI-12/04). (B) Male (MHNG, sample VMI-12/07). (C) Female (MHNG, sample VMI-12/04). Abbreviations: blf = basal lobe, fixed finger, bnm = basal notch, movable finger, ml = median lobe, slm = suprabasal lobe, movable finger, snf = suprabasal notch, fixed finger. Scale, 1 mm.

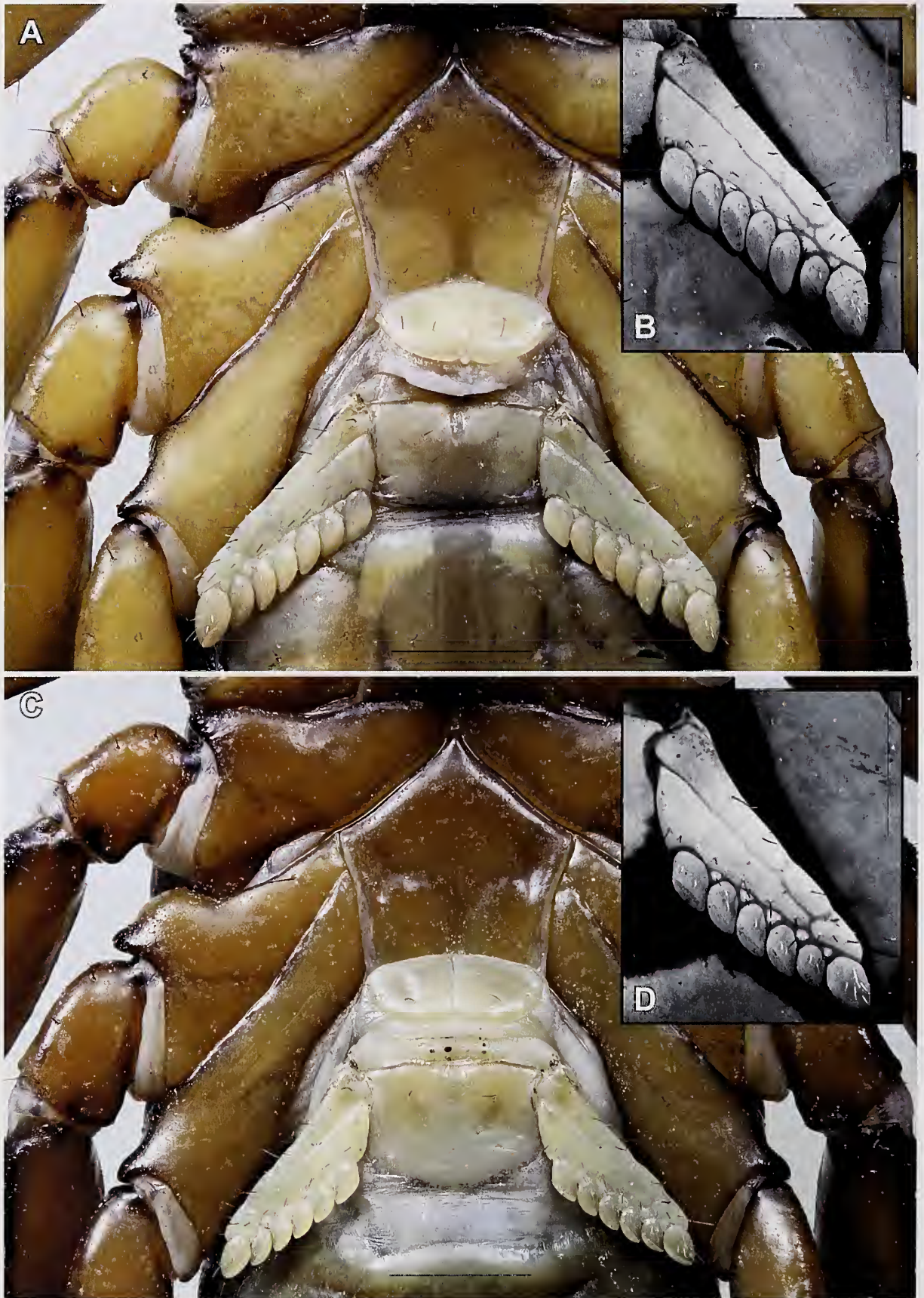


Fig. 8. *Hormiops davidovi* Fage, 1933, coxae of legs II-IV, sternum, genital operculum and pectines, ventral aspect (A, C), left pectine under UV light (B, D). (A-B) Male (MHNG, sample VMI-12/04). (C-D) Female (MHNG, sample VMI-12/04). Scales, 1.5 mm (A, C), 1 mm (B, D).

not surpassing distal edge of leg IV coxa (Fig. 8A); fulcra and three marginal lamellae present (Fig. 8B). Pectinal teeth count 7/7; teeth short, straight, only covered with sensory papillae distally.

Mesosoma: Tergites I to VII gradually decreasing in width. Posterior margins of pre-tergites I-VII smooth (Fig. 4A, E). Post-tergites: posterior margins of I-VI sublinear, without distinct prominence (Fig. 4A, E); lateral transversal sulcus absent or vestigial (shallow) on I-IV; intercarinal surfaces of I-VII finely and densely granular (creating a matte appearance), even, without reticulated network of ridges and dimples. Respiratory stigmata (spiracles) of sternites IV-VI short (less than one third of sternite width) and crescent-shaped, with distinct curve. Sternite VII acarinate.

Metasoma: Length similar to that of female (Tab. 1); intercarinal surfaces smooth, with sparse minute granules. Segment I flattened dorso-ventrally (wider than high, wider than following segments, lower than following segments) (Fig. 9B-C); segments II-V laterally compressed (higher than wide); segments I-IV each with median sulcus shallow to absent; dorso-submedian and dorsolateral carinae obsolete; ventrolateral and ventro-submedian carinae distinct at least on some segments. Segment I: dorsomedian posterior spiniform granules weakly developed or absent; posterior spiniform granules of dorso-submedian carinae weakly developed or absent, not noticeably larger than preceding granules; lateral median carina distinct anteriorly; ventrolateral and ventro-submedian carinae converging to same point near posterior margin of segment; ventrolateral carinae each with small spiniform granules posteriorly and none medially; ventro-submedian carinae distinct in anterior half, fused into a single carina in posterior half, with small spiniform granules posteriorly and even smaller granules medially; all granules pointing anteriorly. Segment II: dorsomedian posterior spiniform granules weakly developed or absent; posterior spiniform granules of dorso-submedian carinae weakly developed to absent, not noticeably larger than preceding granules; ventrolateral carinae each with one large spiniform granule posteriorly and with smaller granules scattered subposteriorly and medially; each ventro-submedian carinae with one large and one to two smaller spiniform granules medially, one large spiniform granule sub-posteriorly, and none to two small spiniform granules posteriorly; all granules pointing anteriorly. Segments III and IV: posterior spiniform granules of dorso-submedian carinae distinctly larger than preceding granules; ventrolateral carinae and ventro-submedian carinae weakly developed, smooth, without larger spiniform granules. Segment V: dorsal intercarinal surface smooth; dorsolateral carinae obsolete; ventrolateral carinae distinct, anterior half with small spiniform granules, posterior half with few larger spiniform granules; ventromedian carina expressed only in anterior half, with scattered small granules; anal arch with few large conical spiniform granules; all granules pointing posteriorly.

Telson: Shorter than metasomal segment V (Fig. 9B); vesicle surfaces smooth.

Hemispermatothore and spermatothore (Figs 10-11): Distal lamina slightly curved, longer than basal part; distal crest absent; single laminar hook situated in basal third; basal extrusion absent; transverse ridge distinct, approximately aligned with base of laminar hook, merging with ental edge at base of laminar hook. Capsular lamella thin, folded only proximally and unfolded distally to flattened extremity (tip and base approximately of same width); longitudinal carina on dorsal surface weak to absent; accessory hook and accessory lobe absent; lamellar tip approximately aligned with base of laminar hook, distal to tip of distal lobe. Distal lobe well developed, not hook-like, without accessory hook, carinae or crest. Basal lobe well developed, spoon-shaped, merging with ental process; ectal edge without accessory fold, forming 90° angle with lamella; ental edge without accessory fold toward eetal part, forming 90° angle with lamella.

Book lungs: Lamellar surfaces with regularly spaced, simple trabeculae, each with a knoblike tip (Fig. 12A-B); distal edges of lamellae covered with areolate structures formed by fusion of bent cuticular processes (Fig. 12C, D); posterior edge of spiracle smooth, margin close to atrial wall with hillock-like structures and with chisel-like structures ending in broad, flat tip (Fig. 12E-F).

Description of adult female: Same characters as in male except as follows.

Colouration: Legs darker than in males (Fig. 1C cf. Fig 1A).

Pedipalps: All segments noticeably shorter and more robust than in male (Figs 1C, 3B, D, 5A, F, K). Dentate margins of chela fingers linear or nearly so, i.e. without pronounced lobe and notch (Figs 6C, D, 7C). Prolateral process of patella angled approximately perpendicular to longitudinal axis of segment (Fig. 5F).

Carapace: Surface smooth except for sparsely and finely granular areas along posterior part of lateral margins and median longitudinal sulci (Fig. 4B, D).

Genital operculum: Oval to semi-oval, wider than long, approximately same width as posterior margin of sternum (Fig. 8C); opercular sclerites partly fused, median suture distinct; posterior notch present, at least weakly developed.

Pectines: Short, distal edge not reaching distal edge of coxa IV (Fig. 8C). Pectinal teeth count 6/6; areas of teeth covered with sensory papillae smaller than in males (Fig. 8D).

Mesosoma: Post-tergites: lateral transversal sulcus on III-VI slightly deeper than in male (Fig. 4B, F cf. Fig. 4A, E); intercarinal surfaces of I-II smooth, weakly granular laterally; intercarinal surfaces of III-VI smooth, weakly granular laterally and in submedian sulci; intercarinal surfaces of VII smooth, with few minute granules scattered along posterior half of lateral margins.

Metasoma: Intercarinal surfaces smooth (Fig. 9A).

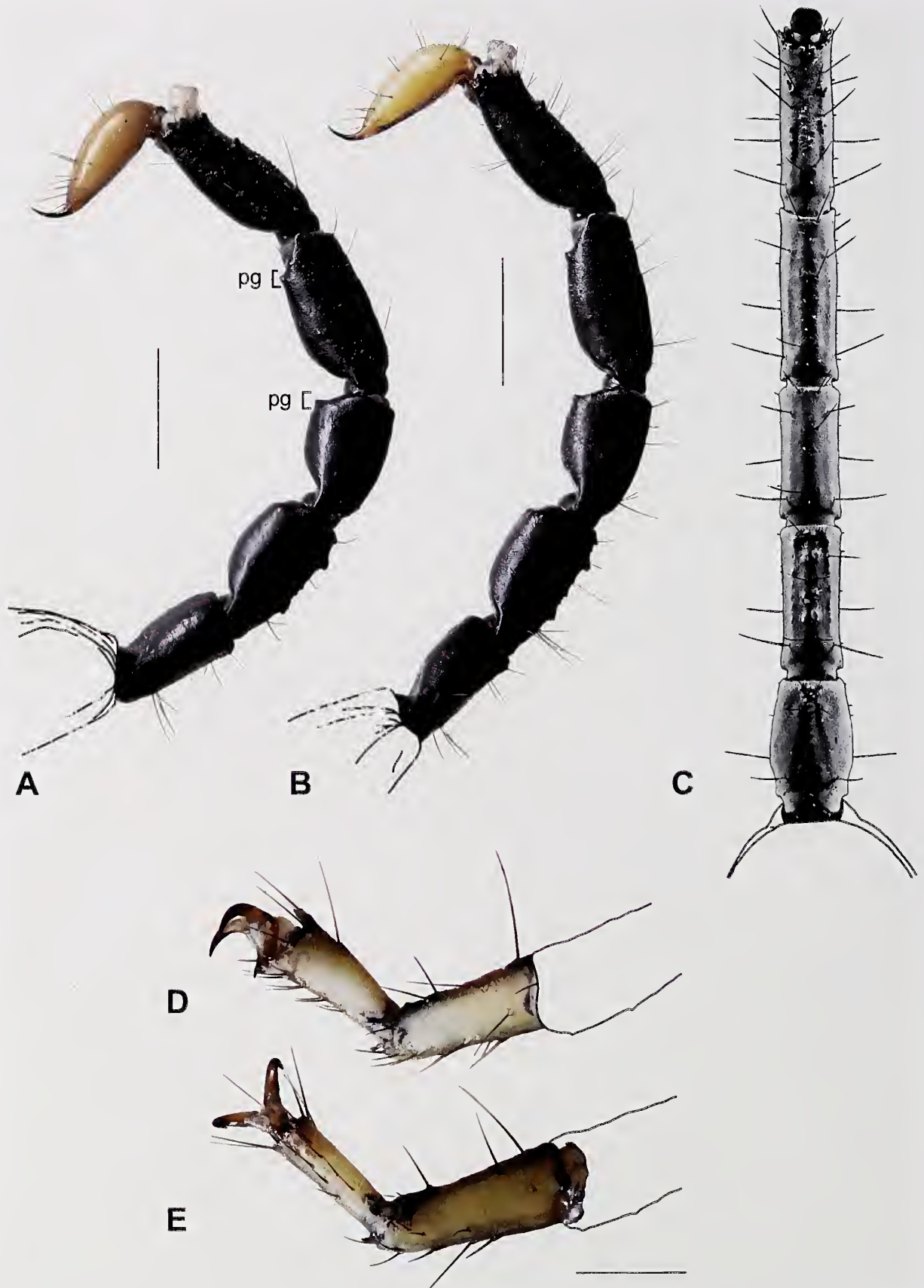


Fig. 9. *Hormiops davidovi* Fage, 1933, metasoma and telson, lateral (A-B) and ventral (C) aspects; left tarsus IV, retrolateral (D) and ventral (E) aspects. (A) Female (MHNG, sample VMI-12/04). (B-E) Male (MHNG, sample VMI-12/04). Abbreviation: pg = posterior granules, dorso-submedian carinae. Scale, 2 mm (A-C), 1 mm (D-E).

Sexual dimorphism: The pedipalps of males and females are strongly dimorphic (Figs 1A, C, 3, 5). They differ between the sexes not only in length compared to body size, but also in allometric slopes (Fig. 13A; *H₀*: slopes are equal, likelihood ratio statistic: 4.279, P-value = 0.038587). Pedipalps are positively allometric in males (slope = 1.618793; lower limit = 1.227101, upper limit = 2.135513; *H₀*: slope not different from 1, test statistic: $r = 0.8025$, P-value = 0.0029489), whereas in females they are isometric (slope = 1.1532493, lower limit = 0.9662842, upper limit = 1.37639; *H₀*: slope not different from 1, test statistic: $r = 0.3514$, P-value = 0.10882).

Intraspecific variation: Large males have proportionally longer pedipalps than small males, as indicated by the positive allometry (Fig. 13A). The development of the suprabasal lobe of the movable finger and of the corresponding suprabasal notch in the fixed finger also varies among males. The suprabasal lobe can be reduced to a low, barely visible hump, or it can even be absent (dentate margins of pedipalp chela fingers thus being straight) in some specimens (Fig. 7B), usually the smaller ones. Pectinal teeth count varies from 6 to 7 in males ($n = 11$, mode = 7) and females ($n = 22$; mode = 6).

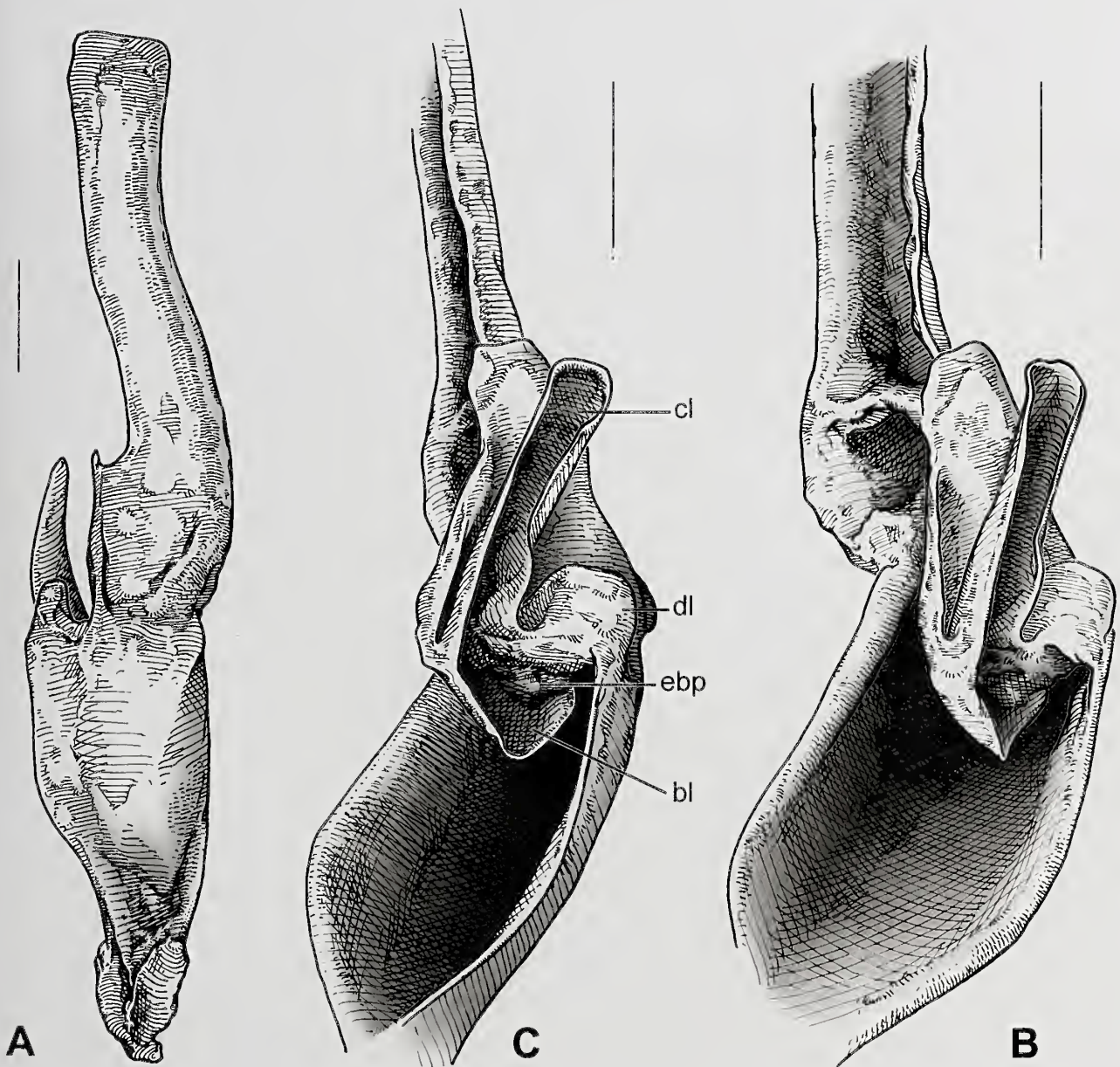


Fig. 10. *Hormiops davidovi* Fage, 1933, male (MHNG, sample VMI-12/04), left hemispermatophore. (A) Dorsal aspect. (B-C) Detail of capsular region, ental (B) and ventral (C) aspects. Abbreviations: bl = basal lobe, cl = capsular lamella, dl = distal lobe, ebp = ental basal process. Scale, 0.5 mm.

Distribution and ecology: *Hormiops davidovi* is only known from, and probably endemic to, the Côn Đảo Archipelago, a group of granitic islands near the southern tip of Vietnam (Fig. 14). Specimens were collected from narrow rock crevices of granitic outcrops in primary evergreen forests (Fig. 15). The habitat and habitus are consistent with the lithophilous ecomorphotype (Prendini, 2001).

Conservation status: The known populations of *H. davidovi* are located on several protected islands that are part of the Côn Đảo National Park. The land area of these islands represents less than 80 km², which designates *H. davidovi* as a short-range endemic, i.e. a species with a distribution area of less than 10,000 km² (Harvey, 2002; Monod & Volschenk, 2004). Although currently not threatened by habitat destruction,

H. davidovi is vulnerable to potential threats from tourism and loss of habitat in the future given its restricted distribution range. It is thus recommended that *H. davidovi* be placed on the IUCN Red List of near threatened species (International Union for the Conservation of Nature, 2001).

***Hormiops infulcra* Monod, 2014**

Figs 1B, D, 13B, 16-28, Tab. 2

Hormiops davidovi. – Kovařík, 2000: 57-58, figs 1-7. [mis-identification]

Hormiops infulcra. – Monod, 2014: 602-603, figs 1b, d, 2b, 3c, e, h, i.

Material: *Holotype:* MHNG; male; sample VMI-12/14, Peninsular Malaysia, Pahang, Pulau Tioman, trail from

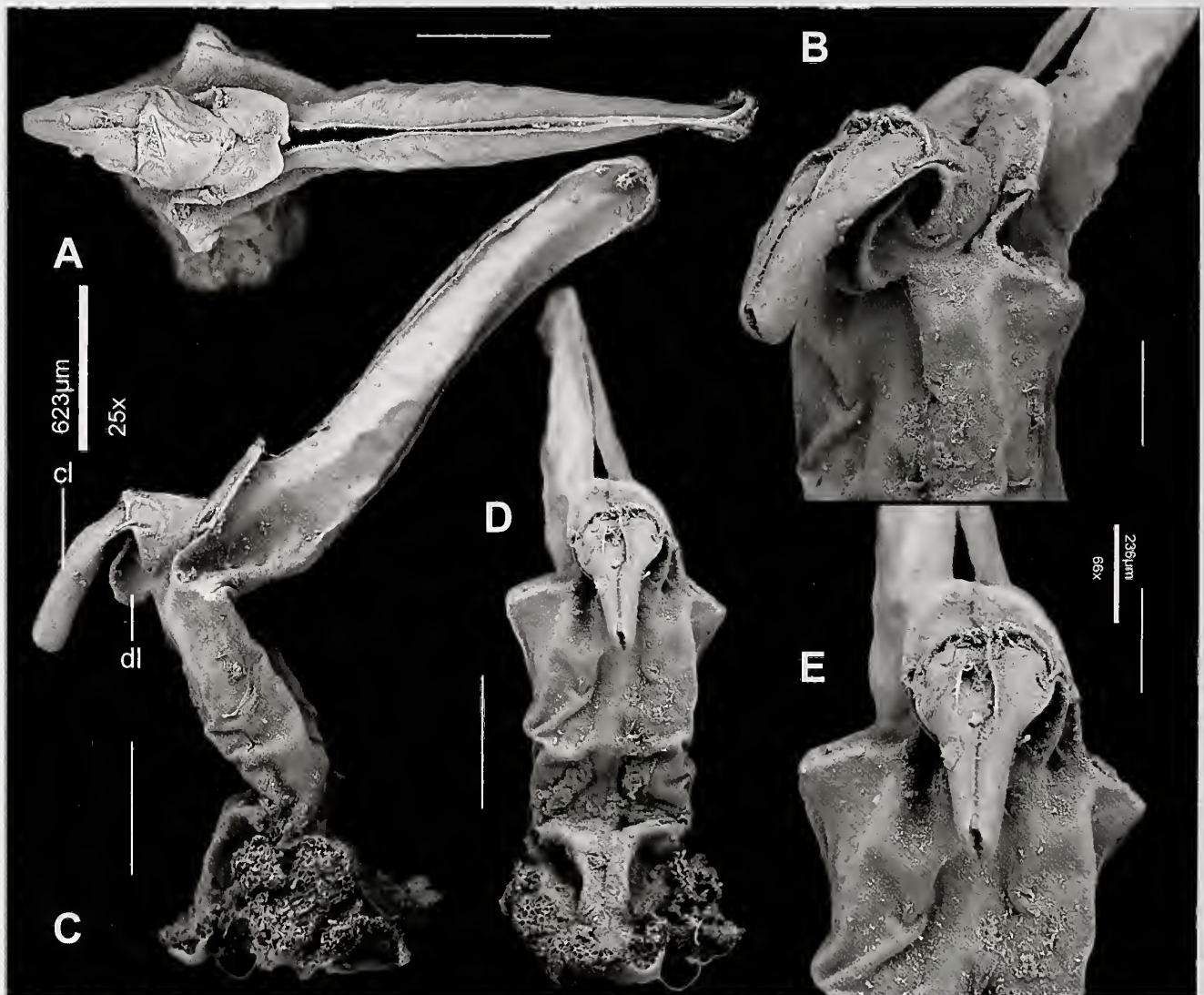


Fig. 11. *Hormiops davidovi* Fage, 1933, male (MHNG, sample VMI-12/01), post-insemination spermatophore. In toto, upper (A), lateral (C), and anterior (D) aspects. Detail of capsular region, rotated approximately 45° counter-clockwise from lateral aspect (B), anterior aspect (E). Abbreviations: cl = capsular lamella, dl = distal lobe. Scales, 0.5 mm (A, C-D), 0.25 mm (B, E).

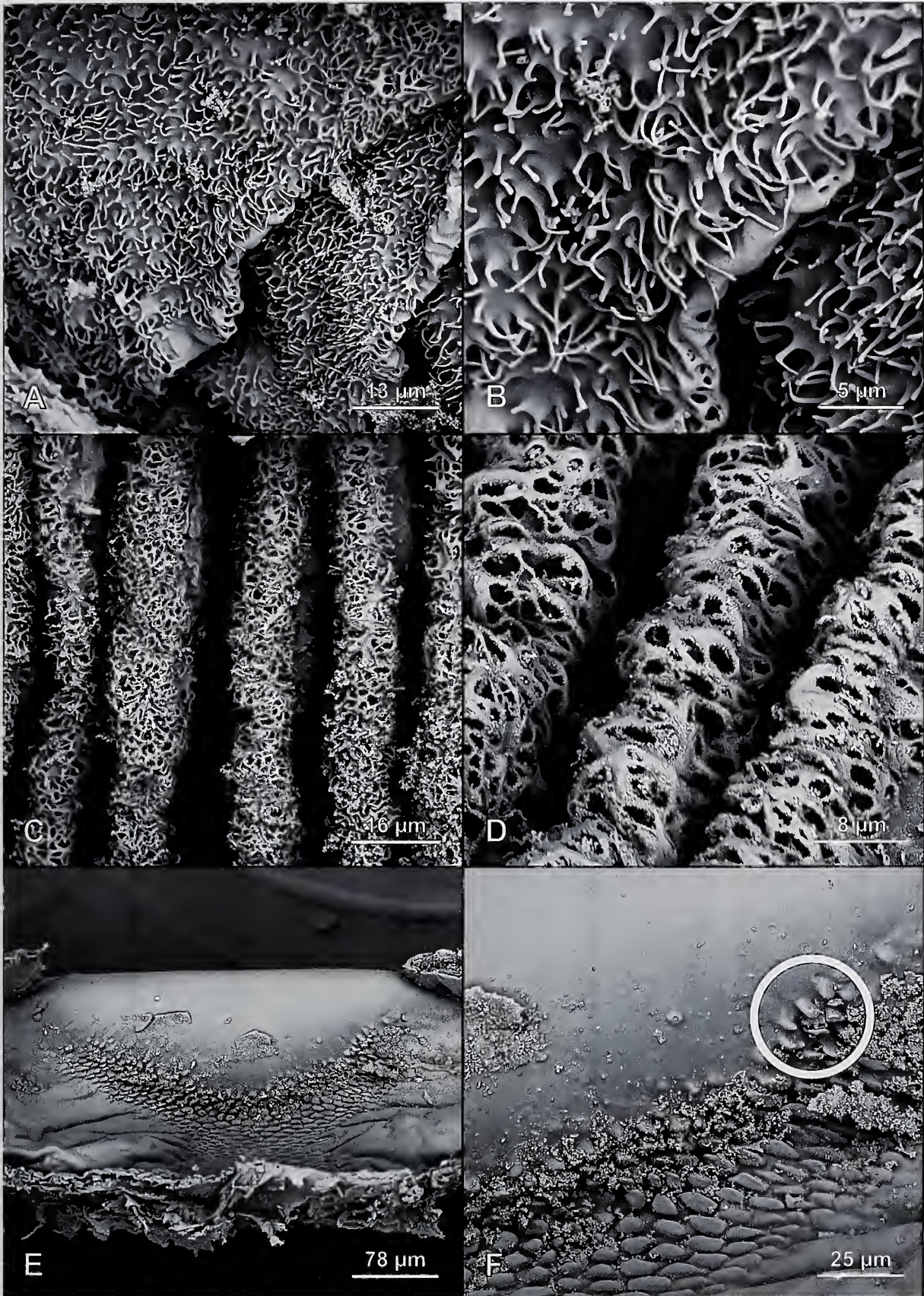


Fig. 12. *Hormiops davidovi* Fage, 1933, female (MHNG, sample VMI-12/04), book lungs. (A-B) Surface of book lung lamella with simple trabeculae. (C-D) Arcuate distal edges of book lung lamellae, posterior view. (D-E) Movable posterior edge of spiracle with hillock-like and chisel-like (circle) structures, anterior view.

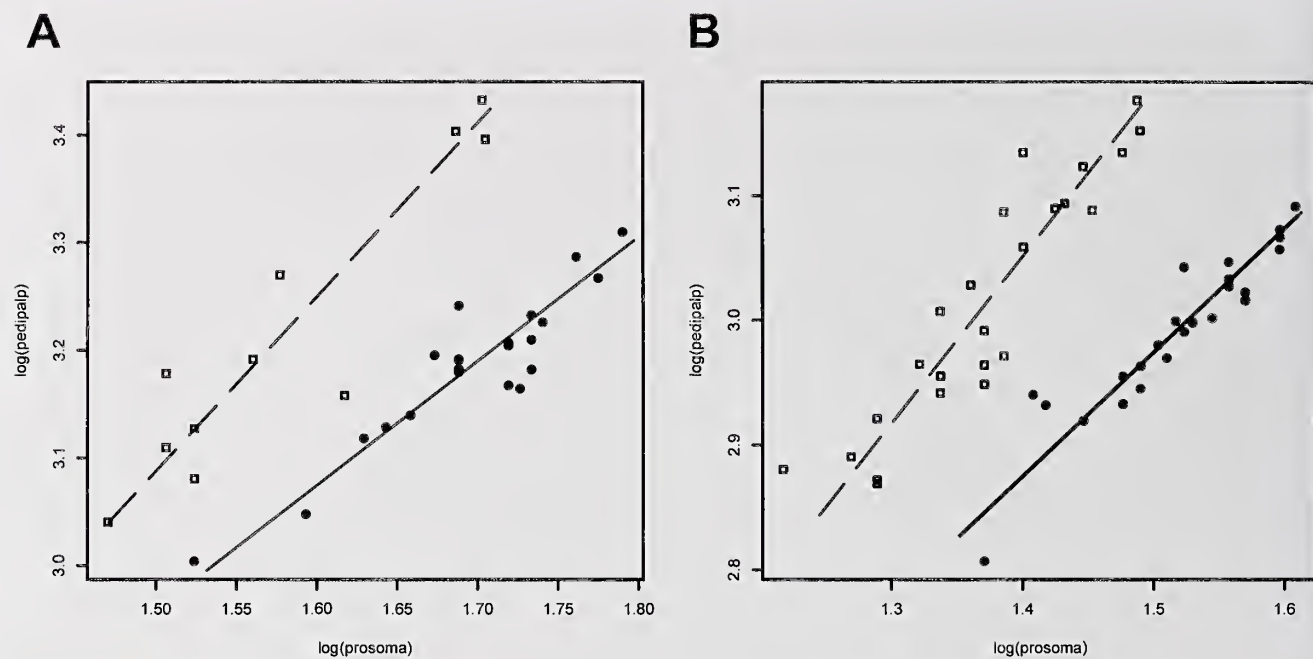


Fig. 13. Bivariate scatter plots of the pedipalp size (Y) versus body size (X) with fitted SMA lines for males (dashed lines, squares) and females (full lines, filled circles). (A) *Hormiops davidovi* Fage, 1933. (B) *Hormiops infulcra* Monod, 2014.

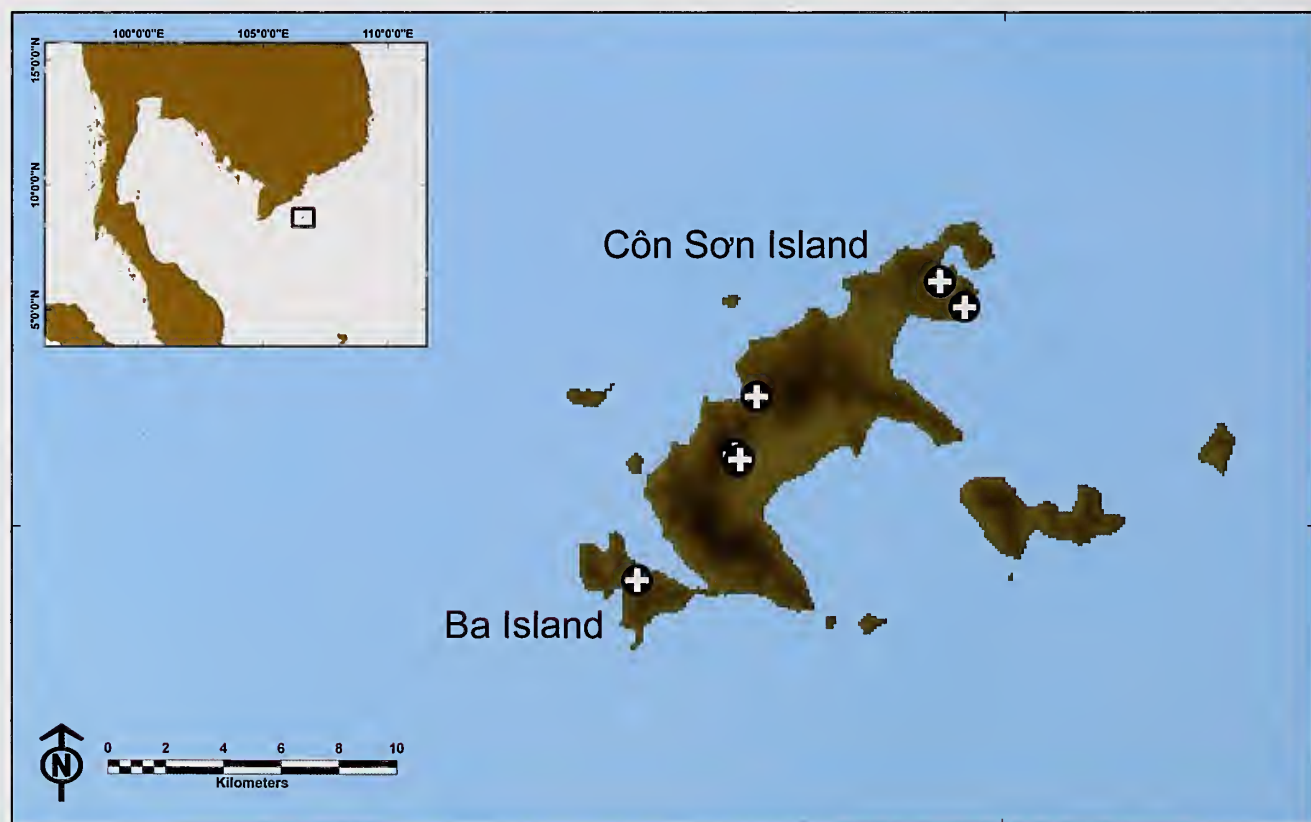


Fig. 14. Known localities of *Hormiops davidovi* Fage, 1933 in the Côn Đảo Archipelago, Vietnam, with topography indicated.



Fig. 15. Habitat of *Hormiops davidovi* Fage, 1933 on Côn Sơn Island, Côn Đảo Archipelago, Vietnam.

Kampung Genting to Paya, N2°46' E104°07'; 70 m, rainforest, in rock crevices; 25.I.2012; leg. L. Monod.

Paratypes: MHNG; 3 males, 2 females, 5 juv.; same data as for holotype. – MHNG; 10 males, 13 females, 46 juv.; Pulau Tioman, foothills of Gunung Kajang, N2°47' E104°07'; 60 m, rainforest, in rock crevices; 1-2.X.2001; leg. L. Monod. – MHNG; 4 males, 7 females, 14 juv.; sample VMI-12/12, Pulau Tioman, trail near Kampung Mukut, N2°44' E104°07'; 115 m, rainforest, in rock crevices; 23.I.2012; leg. L. Monod. – MHNG; 4 males, 2 females, 2 juv.; sample VMI-12/13, Pulau Tioman, trail near Nipah, N2°45' E104°07'; 25 m, rainforest, in rock crevices; 24.I.2012; leg. L. Monod. – MHNG; 2 males, 1 female; sample VMI-12/15, Pulau Tioman, trail from Japamala Resort to Kampung Lanting, N2°44' E104°07'; 65 m, rainforest, in rock crevices; 27.I.2012; leg. L. Monod.

Other material: LKCM, ZRC.ARA.456; 1 female, 4 juv.; Peninsular Malaysia, Pahang, Pulau Tulai [N2°54'44" E104°06'26"]; 23.VIII.2003; leg. P. K. L. Ng *et al.* – LKCM, ZRC.ARA.457; 1 juv.; same data as ZRC.ARA.456.

Diagnosis: *Hormiops infulcra* differs from *H. davidovi* by the following combination of characters. *Hormiops infulcra* is distinctly smaller and slightly lighter in colour than *H. davidovi* (Fig. 1). The carapace of males is slightly less densely granular in *Hormiops infulcra* (Fig. 18A, C) than in *H. davidovi* (Fig. 4A, C). The exteroventral carinae of the pedipalp femur is finely granular in *H. infulcra* (Fig. 19M-N), whereas it bears coarse spiniform granules in *H. davidovi* (Fig.

5M-N). The dorsoexternal carina of the pedipalp patella in *H. infulcra* is costate-granular (Fig. 19G-H) and more distinct than the faint costate ridge observed in *H. davidovi* (Fig. 5G-H). The digital earina of the pedipalp chela is granular in *H. infulcra* (Fig. 19B-C), whereas it is costate in *H. davidovi* (Fig. 5B-C). In males of *H. infulcra* the dentate margins of the fixed and movable chela fingers are linear (Fig. 20A-B, 21A), whereas most males of *H. davidovi* possess a well-developed suprabasal lobe on the movable finger and a corresponding suprabasal notch on the fixed finger (Fig. 6A-B, 7A-B). The telotarsus IV has four proventral macrosetae in *Hormiops infulcra* (Fig. 23D-E), whereas they bear five in *H. davidovi* (Fig. 9D-E). In *Hormiops infulcra* the average number of pectinal teeth is six for males and five for females (Fig. 22), whereas males and females of *H. davidovi* usually have seven and six pectinal teeth respectively (Fig. 8). The pectinal fulcræ are absent in *H. infulcra* (Fig. 22), but present in *H. davidovi* (Fig. 8). The tergites of males are medially less granular in *H. infulcra* (Fig. 18A, E) than in *H. davidovi* (Fig. 4A, E). Moreover, in *H. infulcra* males, the posterior margins of tergites I-V are smooth medially and the median ridges are sometimes smooth as well (Fig. 18A, E), whereas in *H. davidovi* males the tergites are completely granular (Fig. 4A, E). The metasoma is finely and sparsely granular in *H. infulcra* (Fig. 23A-C), whereas in *H. davidovi* it is smooth or nearly so (Fig. 9A-C). The ventrosubmedian carinae of metasomal segment II have no granules posteriorly in *H. infulcra* (Fig. 23C), whereas in most specimens of *H. davidovi* they bear two small posterior

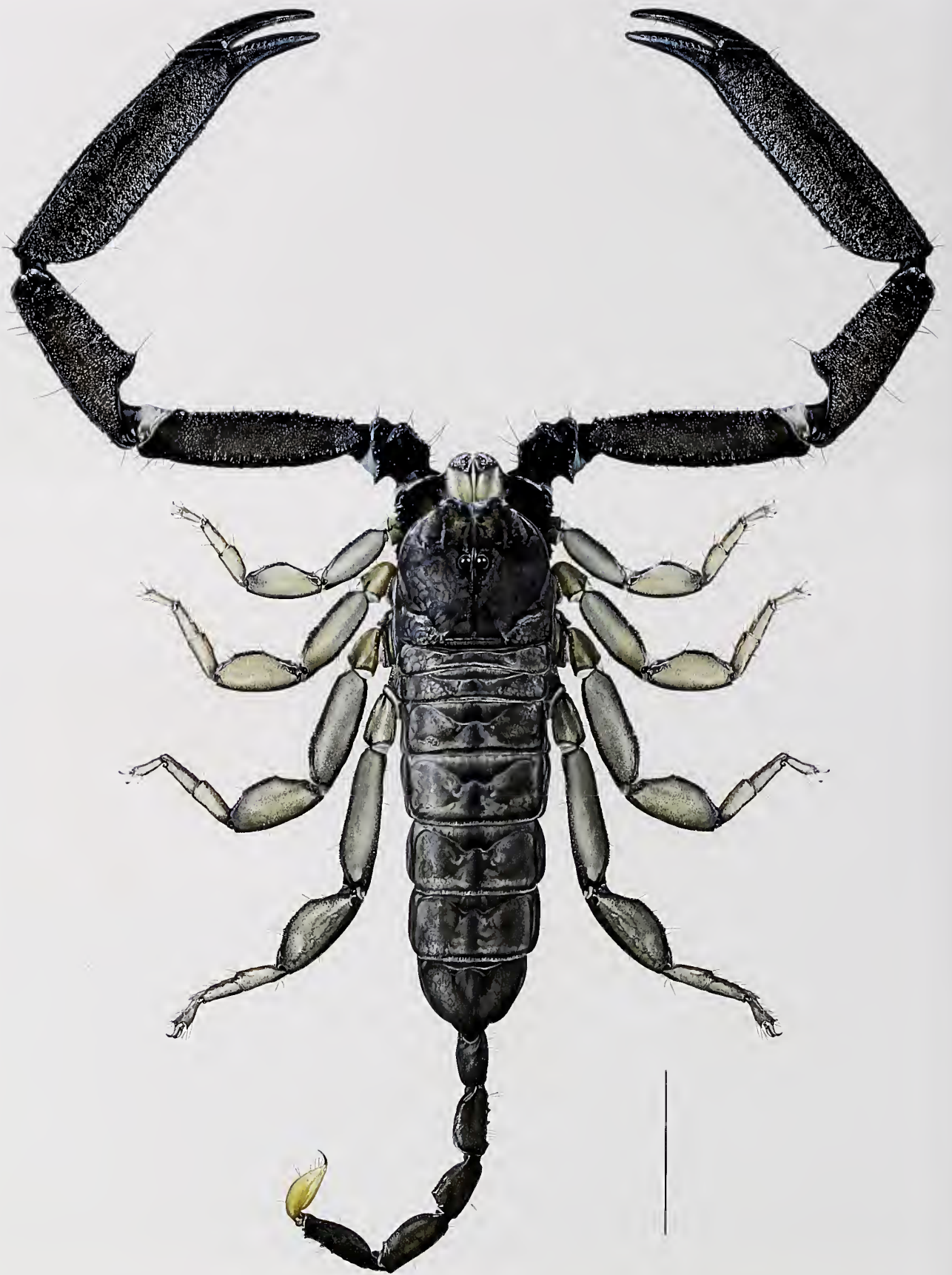


Fig. 16. *Hormiops infulcra* Monod, 2014, habitus of male, dorsal aspect, reconstruction based on scientific illustrations and photographs of live specimens. Scale, 5 mm.



Fig. 17. *Hormiops infulcra* Monod, 2014, habitus, dorsal (A-B) and ventral (C-D) aspects. (A, C) Male holotype (MHNG, sample VMI-12/14). (B, D) Female paratype (MHNG, sample VMI-12/14). Scale, 5 mm.

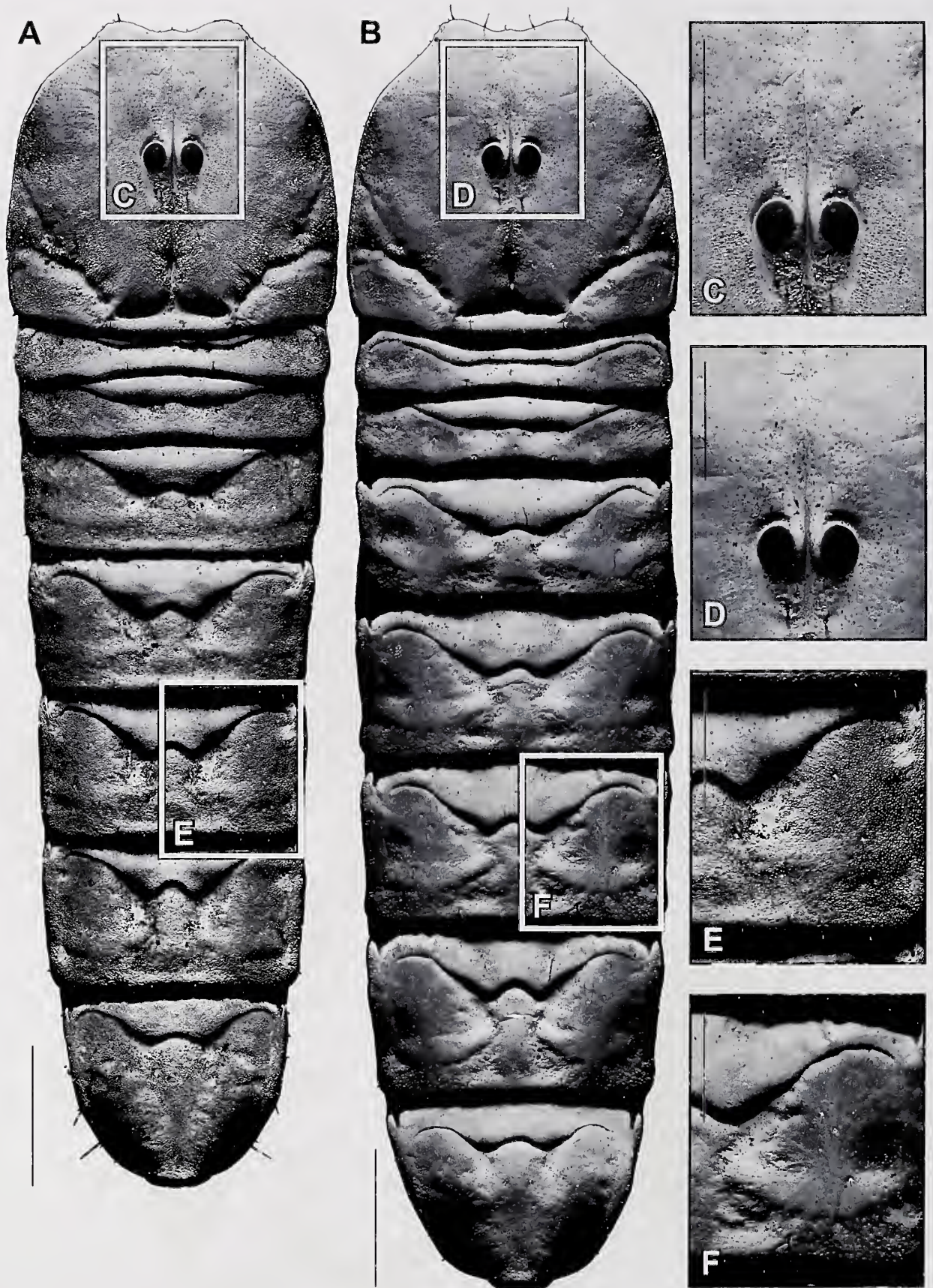


Fig. 18. *Hormiops infulcra* Monod, 2014, carapace and mesosomal tergites showing ornamentation and macrosculpture of cuticle (A-B), with detailed view of carapace (C-D) and tergite V (E-F), dorsal aspect. (A, C, E) Male holotype (MHNG, sample VMI-12/14). (B, D, F) Female paratype (MHNG, sample VMI-12/14). Scale, 2 mm (A-B), 1 mm (C-F).



Fig. 19. *Hormiops infulcra* Monod, 2014, pedipalp chela (A-E), patella (F-J), femur and trochanter (K-O), dorsal (A-B, F-G, K-L), retrolateral (C, H, M), ventral (D, I, N) and prolateral (E, J, O) aspects showing trichobothrial pattern. (A, F, K) Female paratype (MHNG, sample VMI-12/14). (B-E, G-J, L-O) Male holotype (MHNG, sample VMI-12/14). Scale, 2 mm.

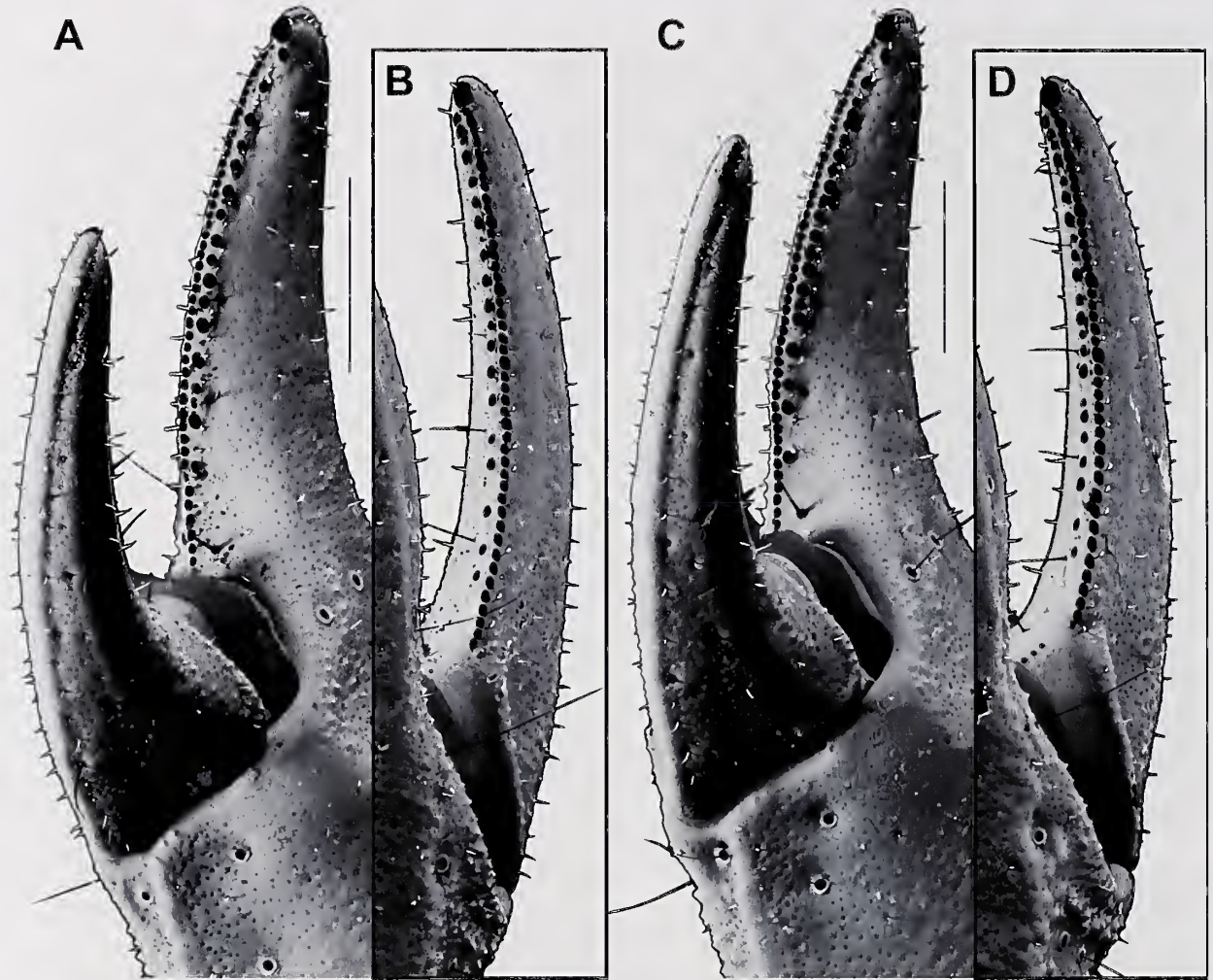


Fig. 20. *Hormiops infulcra* Monod, 2014, pedipalp chela, dentate margins of fixed (A, C) and movable (B, D) fingers. (A-B) Male holotype (MHNG, sample VMI-12/14). (C-D) Female paratype (MHNG, sample VMI-12/14). Scale, 1 mm.

spiniform granules (Fig. 9C). The distal lamina of the hemispermatophore is straight and only slightly longer than the basal part in *H. infulcra* (Figs 24A, 25A), whereas in *H. davidovi* it is slightly curved and longer than the basal part (Figs 10A, 11C).

Description of adult male: *Colouration:* Dorsal surface of chelicera manus orange-brown, with darker infuscation; fingers dark brown to black (Figs 1B, 16). Carapace reddish brown, with darker infuscations, tergites brown. Pedipalps reddish brown, with darker infuscation; carinae and fingers black. Legs orange brown to light brown, prolateral carinae of femora black. Coxapophyses, sternum, genital operculum and pectines yellowish to orange-brown. Metasoma brown, with darker infuscations. Telson yellow, aculeus reddish black. *Cuticle:* Non-granular surfaces of carapace, pedipalps and legs, mesosoma and metasoma finely punctate.

Carapace: Anterior margin with shallow median notch (Fig. 18A). Anterior furcated suture and sulci vestigial. Median ocular tubercle situated anteromedially, very

low, small, occupying about one ninth of carapace width; superciliary carinae absent; median ocelli present, at least twice the size of lateral ocelli, separated by at least half the diameter of median ocellus. Two pairs of lateral ocelli, equal in size, equidistant and adjacent to one another. Postocular carapace margin without spines or tubercles. Surfaces finely and densely granular, giving tegument a matte appearance, except for anterior and median areas; anterolateral surfaces and frontal lobes smooth; median surface smooth, finely and densely granular around ocular tubercle (Fig. 18A, C).

Chelicerae: Median and basal teeth of fixed finger fused into a bicuspid. Dorsal margin of movable finger with four teeth (one subdistal and one basal); dorsal distal tooth smaller than ventral distal tooth; ventral margin smooth.

Pedipalps: Segments long and slender (Figs 1B, 16, 17A, C, 19B-E, G-J, L-O), with femur length approximately 1.5 times carapace length (Tab. 2). Chela almost asetose. Chela fingers: Dentate margins of fixed and movable fingers linear (without pronounced lobe and notch), with



Fig. 21. *Hormiops infulcra* Monod, 2014, pedipalp chela, retrolateral aspect showing dentate margin of chela fingers. (A) Male holotype (MHNG, sample VMI-12/14). (B) Female paratype (MHNG, sample VMI-12/14). Scale, 1 mm.

two rows of primary denticles, these rows merged to each other basally, accessory denticles absent, median row with few slightly larger denticles (Figs 20A-B, 21A).

Pedipalp earinae: Femur (Fig. 19L-O): internomedian ventral carina vestigial, comprising two large spiniform granules situated proximally and medially on article; internomedian dorsal carina obsolete, without granules; dorsointernal carina coarsely granular, more strongly developed than dorsoexternal carina; dorsoexternal carina coarsely granular, slightly less granular distally; ventroexternal carina granular; ventromedian carina obsolete; ventrointernal carina with coarse spiniform granules. Patella (Fig. 19G-J): prolateral dorsal and prolateral ventral spiniform processes equally developed and fused medially forming a prominent median spine, angled approximately 45° relative to longitudinal axis of segment; internodorsal carina with coarse spiniform granules; dorsomedian carinae granular proximally and medially, obsolete medially; dorsoexternal carina distinct and costate-granular; externomedian carina granular; ventroexternal carina distinct, smooth to costate; ventrointernal carina with coarse spiniform granules. Chela manus (Fig. 19B-E): internomedian

carina granular; dorsal secondary carina obsolete; digital carina distinct, granular, more strongly developed than external secondary carina; external secondary carinae obsolete; ventroexternal carina costate; ventromedian and ventrointernal carinae obsolete.

Pedipalp surface macrosculpture: Femur (Fig. 19L-O): dorsal intercarinal surface faintly granular in proximal part and on retrolateral edge; retrolateral intercarinal surface granular; ventral intercarinal surface granular, distal extremity smooth; prolateral intercarinal surface finely granular. Patella (Fig. 19G-J): dorsal intercarinal surface faintly granular, distal extremity smooth; retrolateral intercarinal surface smooth; retrolateral dorsal intercarinal surface smooth; ventral intercarinal surface smooth, prolateral edge faintly granular; prolateral intercarinal surface finely granular, with distal extremity smooth. Chela (Fig. 19B-E): dorsal intercarinal surface with scattered granules fused into a reticulated network, becoming denser along prolateral and retrolateral edges; retrolateral intercarinal surface granular; ventral intercarinal surface faintly granular (anamostosed granules), smooth medially and distally; prolateral intercarinal surface granular, distal extremity

smooth. Chela fingers smooth; surface around *db*, *dsb* and *dst* trichobothria of fixed finger smooth.

Trichobothriotaxy: Pedipalp orthobothriotaxic, accessory trichobothria absent (Figs 19B-E, G-J, L-O). Patella: *d*₂ situated distal to patellar process; five *eb* trichobothria; two *esb* trichobothria; two *em* trichobothria; one *est* trichobothrium; three *et* trichobothria; three *V* trichobothria. Chela manus with *Dt* situated in proximal third; *Eb*₃ situated close to *Eb*_{1,2}; *Esb* basal, aligned with *Eb* series; *Est* situated at or near midpoint; four *V* trichobothria, with *V*₃ and *V*₄ clearly separated. Chela fixed finger with *db* situated on dorsal surface; *esb*, *eb*, *est* and *et* equidistant; *eb* situated at base of finger, proximal to point of articulation between fixed and movable fingers, above *esb-et* axis; *esb* situated at base of finger, proximal to point of articulation between fixed and movable fingers, below *est-et* axis; two *i* trichobothria proximal to base of fixed finger.

Coxosternal region: Leg III coxae without swelling or bulge anterodistally. Sternum equilateral pentagonal (Fig. 22A); anterior width slightly greater than posterior width; length slightly greater than posterior width.

Legs: Femora I-IV with ventral surfaces bearinate, proventral and retroventral carinae granular. Retroventral margins of tibiae I and II without setiform macrosetae. Pro- and retrolateral margins of basitarsi I-IV each with four setiform macrosetae. Telotarsi I-IV: pro/retroventral margins each with 4/5, 4/5, 4/5 and 4/5 setiform macrosetae (Fig. 23D-E); ventromedian row of spinules absent; dorsomedian lobe pronounced; laterodistal lobes truncate; ungues curved, shorter than telotarsus.

Genital operculum composed of two subtriangular sclerites (Fig. 22A).

Pectines: Moderately elongated, distal edge reaching but not surpassing distal edge of leg IV coxa (Fig. 22A); fulcrum absent, two marginal lamellae (Fig. 22B). Pectinal teeth count 6/6; teeth short, straight, only covered with sensory papillae distally.

Mesosoma: Tergites I to VII gradually decreasing in width. Posterior margins of pre-tergites I-VII smooth (Fig. 18A, E). Post-tergites: posterior margins of I-VI sublinear, without distinct prominence (Fig. 18A, E); lateral transversal sulcus absent or vestigial (shallow) on I-IV; intercarinal surfaces of I-VII even, without reticulated network of ridges and dimples; intercarinal surfaces of I finely and densely granular laterally, smooth medially; intercarinal surfaces of II-VI finely and densely granular (creating a matte appearance), posterior margin smooth medially, ridges weakly granular to smooth; intercarinal surface of VII finely and densely granular (creating a matte appearance). Respiratory stigmata (spiracles) of sternites IV-VI short (less than one third of sternite width) and crescent-shaped, with distinct curve. Sternite VII acarinate.

Metasoma: Length similar to that of female (Tab. 2); intercarinal surfaces sparsely and finely granular. Segment I flattened dorso-ventrally (wider than high,

wider than following segments, lower than following segments) (Fig. 23B-C); segments II-V compressed laterally (higher than wide); segments I-IV each with median sulcus shallow to absent; dorso-submedian and dorsolateral carinae obsolete; ventrolateral and ventro-submedian carinae distinct at least on some segments. Segment I: dorsomedian posterior spiniform granules weakly developed or absent; posterior spiniform granules of dorsosubmedian carinae weakly developed to absent, not noticeably larger than preceding granules; lateral median carina distinct anteriorly; ventrolateral and ventro-submedian carinae converging to same point near posterior margin of segment; ventrolateral carinae each with small spiniform granules posteriorly and none medially; ventro-submedian carinae distinct in anterior half, fused into a single earina in posterior half, with small spiniform granules posteriorly and even smaller granules medially; all granules pointing anteriorly. Segment II: dorsomedian posterior spiniform granules weakly developed or absent; posterior spiniform granules of dorso-submedian carinae weakly developed to absent, not noticeably larger than preceding granules; ventrolateral carinae each with one large spiniform granule posteriorly, plus smaller granules scattered subposteriorly and medially; each ventrosubmedian earina with one to three large spiniform granules medially, one large spiniform granule sub-posteriorly, and no spiniform granules posteriorly; all granules pointing anteriorly. Segments III-IV: posterior spiniform granules of dorso-submedian carinae distinctly larger than preceding granules; ventrolateral and ventrosubmedian carinae weakly developed, densely and finely granular. Segment V: dorsal intercarinal surface smooth; dorsolateral carinae obsolete; ventrolateral carinae distinct, anterior half with small spiniform granules, posterior half with few larger spiniform granules; ventromedian carina expressed only in anterior half, with few small granules; anal arch with few large conical teeth; all granules pointing posteriorly. *Telson*: Shorter than metasomal segment V (Fig. 23B); vesicle surfaces smooth.

Hemispermaphore and spermaphore (Figs 24, 25): Distal lamina straight or nearly so, slightly longer than basal part; distal crest absent; single laminar hook situated in basal third; basal extrusion absent; transverse ridge distinct, approximately aligned with base of lamellar hook, merging with ental edge distal to laminar hook. Capsular lamella thin, folded only proximally and unfolded distally to flattened extremity (tip and base approximately of same width); longitudinal carina on dorsal surface absent to weak; accessory hook and accessory lobe absent; lamellar tip aligned with base of laminar hook, distal to tip of distal lobe. Distal lobe well developed, not hook-like, without accessory hook, carinae or crest. Basal lobe well developed, spoon-shaped, merging with ental basal process; ectal edge without accessory fold, forming 90° angle with lamella; ental edge without accessory fold toward ectal part, forming 90° angle with lamella.

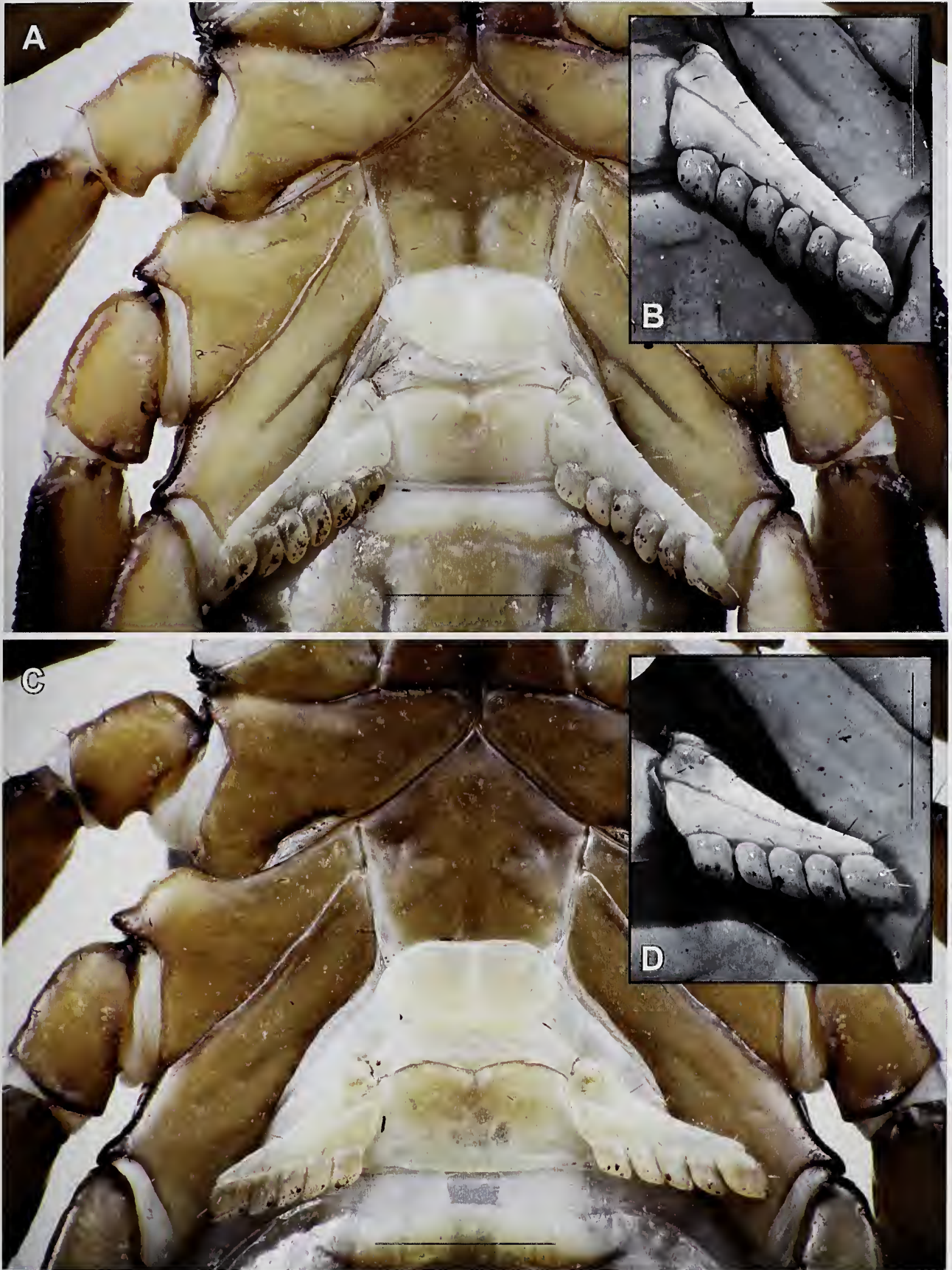


Fig. 22. *Hormiops infulera* Monod, 2014, coxae of legs II-IV, sternum, genital operculum and pectines, ventral aspect (A, C), left pectine under UV light (B, D). (A-B) Male holotype (MHNG, sample VMI-12/14). (C-D) Female paratype (MHNG, sample VMI-12/14). Scales, 1.5 mm (A, C), 1 mm (B, D).

Table 2. *Hormiops infulcra* Monod, 2014, measurements (in mm) of adult males and females.

Status	Holotype		Paratype		Paratype		Paratype		Paratype		Paratype	
	male	VMI-12/14	male	MHNG	male	VMI-12/12	male	MHNG	male	VMI-12/13	male	VMI-12/13
Sex												
Repository	MHNG		MHNG		MHNG		MHNG		MHNG		MHNG	
Registration/sample	VMI-12/14	VMI-12/12	VMI-12/12	VMI-12/13	VMI-12/13	VMI-12/13	VMI-12/13	VMI-12/13	VMI-12/13	VMI-12/13	VMI-12/14	VMI-12/14
Total length	28	24	26	23	27	28	27	28	27	28	31	30
Carapace length	4.4	3.6	3.9	3.4	4	4.6	4.8	4.5	5	5	4.5	5
Carapace anterior width	2.2	1.9	2.1	2	2.2	2.1	2.3	2.4	2.5	2.3	2.4	2.5
Carapace posterior width	4.8	3.9	4.3	3.8	4.3	4.1	5.3	5	5.1	5.1	5	5.8
Femur length	6.5	4.6	5.2	4.8	5.9	4	5	4.9	5	5.1	4.9	5.6
Femur width	1.8	1.4	1.6	1.6	1.7	1.7	1.9	2	2	2	2	2.3
Patella length	6.1	4.5	4.9	4.6	5.6	4.2	5.2	5	5.2	5.2	5	5.6
Patella width	2.3	1.9	2.1	1.8	2.1	2.1	2.6	2.5	2.8	2.8	2.5	2.9
Chela length	11.3	8.5	9.1	8.4	10.3	8.3	10	9.6	10.2	10.2	9.6	10.8
Chela manus width	2.4	2	2.3	2.2	2.3	2.7	3.3	3.1	3.6	3.6	3.1	3.8
Chela manus height	1.5	1.1	1.3	1.4	1.5	1.7	1.6	1.4	1.6	1.6	1.4	1.9
Chela movable finger length	4	3.2	3.8	3.4	3.9	3.5	4.1	4	4.2	4.2	4	4.6
Metasomal segment I length	1.6	1.3	1.4	1.3	1.4	1.1	1.6	1.4	1.3	1.3	1.4	1.6
Metasomal segment I width	1.1	0.9	0.63	0.9	1	1	1.1	1	1.1	1.1	1	1.2
Metasomal segment V length	2.6	2.1	2.4	2.1	2.6	2.1	2.8	2.6	2.4	2.4	2.6	2.8
Metasomal segment V width	0.7	0.6	0.6	0.6	0.6	0.7	0.8	0.7	0.8	0.8	0.7	0.8
Metasomal segment V height	0.9	0.8	0.9	0.7	0.9	0.8	0.9	0.9	1	1	0.9	1
Telson vesicle width	0.8	0.7	0.8	0.7	0.8	0.8	0.8	0.8	0.8	0.8	0.8	0.9
Telson vesicle height	0.8	0.7	0.7	0.7	0.8	0.8	0.9	0.8	0.8	0.8	0.8	0.9

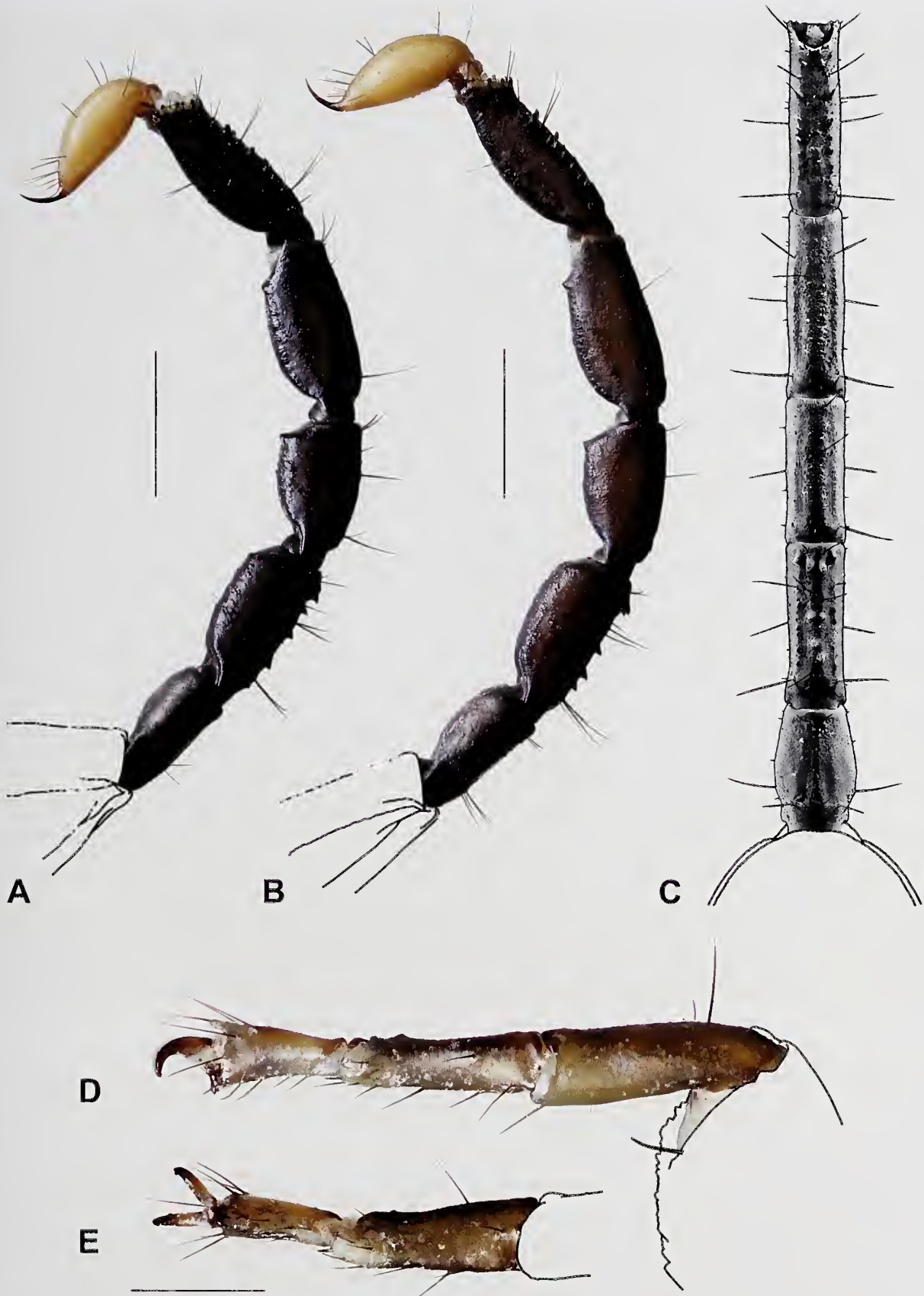


Fig. 23. *Hormiops infulcra* Monod, 2014, metasoma and telson, lateral (A-B) and ventral (C) aspects; left tarsus IV, retrolateral (D) and ventral (E) aspects. (A) Female paratype (MHNG, sample VMI-12/14). (B-E) Male holotype (MHNG, sample VMI-12/14). Scale, 2 mm (A-C), 1 mm (D-E).

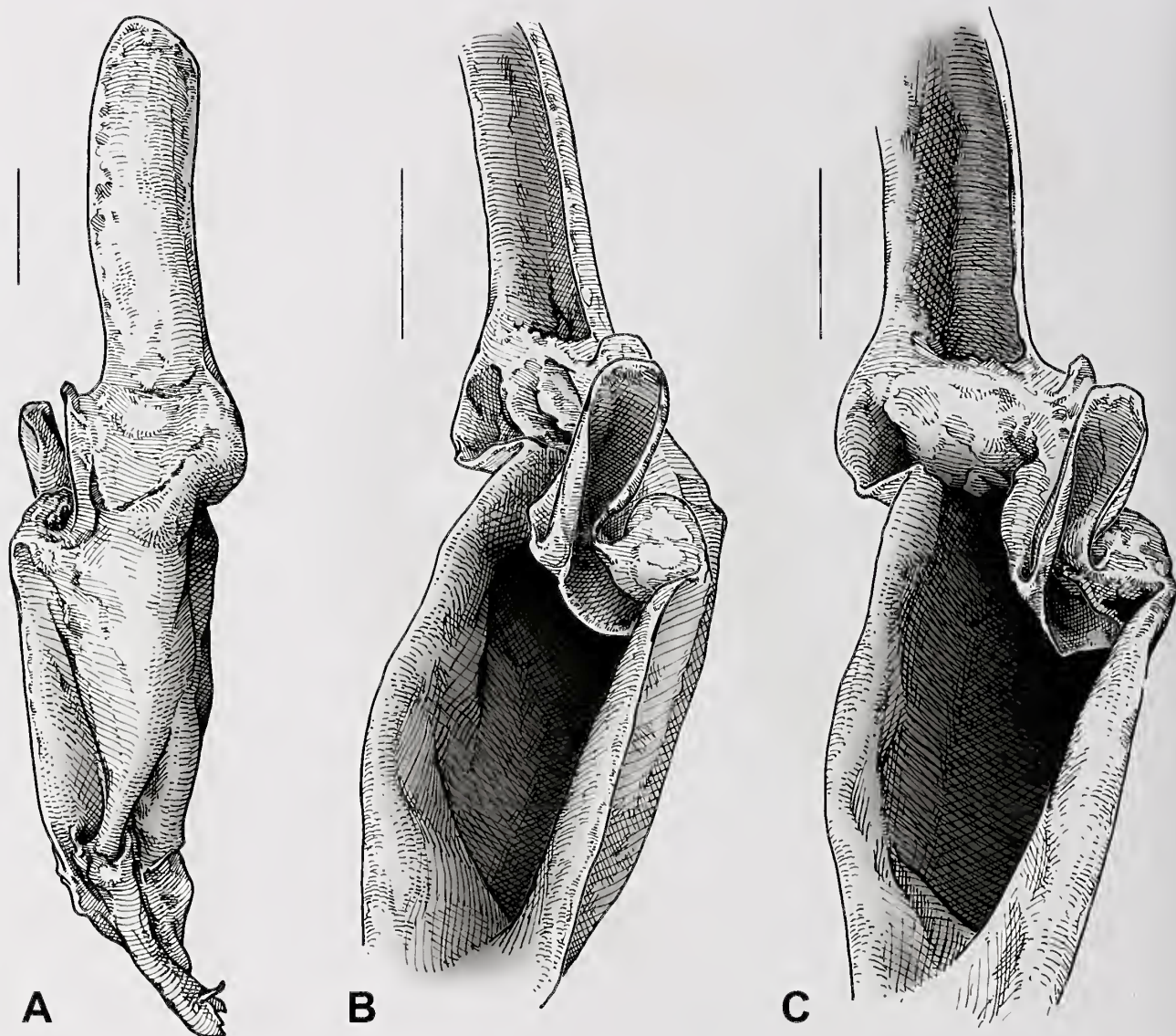


Fig. 24. *Hormiops infulcra* Monod, 2014, male holotype (MHNG, sample VMI-12/14), left hemispermatophore. (A) Dorsal aspect. (B-C) Detail of capsular region, ental (B) and ventral (C) aspects. Scale, 0.5 mm.

Book lungs: Lamellar surfaces with regularly spaced simple trabeculae, each with a knoblike tip (Fig. 26A-B); distal edges of lamellae covered with areuate structures formed by fusion of bent cuticular processes (Fig. 26C-D); posterior edge of spiracle smooth, margin close to atrial wall with hillock-like structures (Fig. 26E-F).

Description of adult female: Same characters as in male except as follows.

Colouration: Pedipalps slightly darker than in males.

Pedipalps: All segments noticeably shorter and more robust than in male (Figs 1D, 17B, D, 19A, F, K). Prolateral process of patella angled approximately perpendicular to longitudinal axis of segment (Fig. 19F).

Carapace: Surface smooth except along posterior part of lateral margins and median longitudinal sulci, sparsely and finely granular (Fig. 18B, D).

Genital operculum: Oval to semi-oval, wider than long, approximately same width as sternum (Fig. 22C); opercular sclerites partly fused, median suture distinct; posterior notch present, at least weakly developed.

Pectines: Short, distal edge not reaching distal edge of coxa IV (Fig. 22C). Pectinal teeth count 5/5.

Mesosoma: Post-tergites: lateral transversal sulcus slightly deeper on III-VI than in male (Fig. 18B, F); intercarinal surfaces of I-III smooth, faintly granular laterally; intercarinal surfaces of IV-VII smooth with few minute granules scattered along lateral margins.

Metasoma: Intercarinal surfaces less granular than in males, almost smooth (Fig. 23A).

Sexual dimorphism: The pedipalps of males and females are strongly dimorphic (Figs 1B, D, 17, 19). They differ between the sexes not only in length

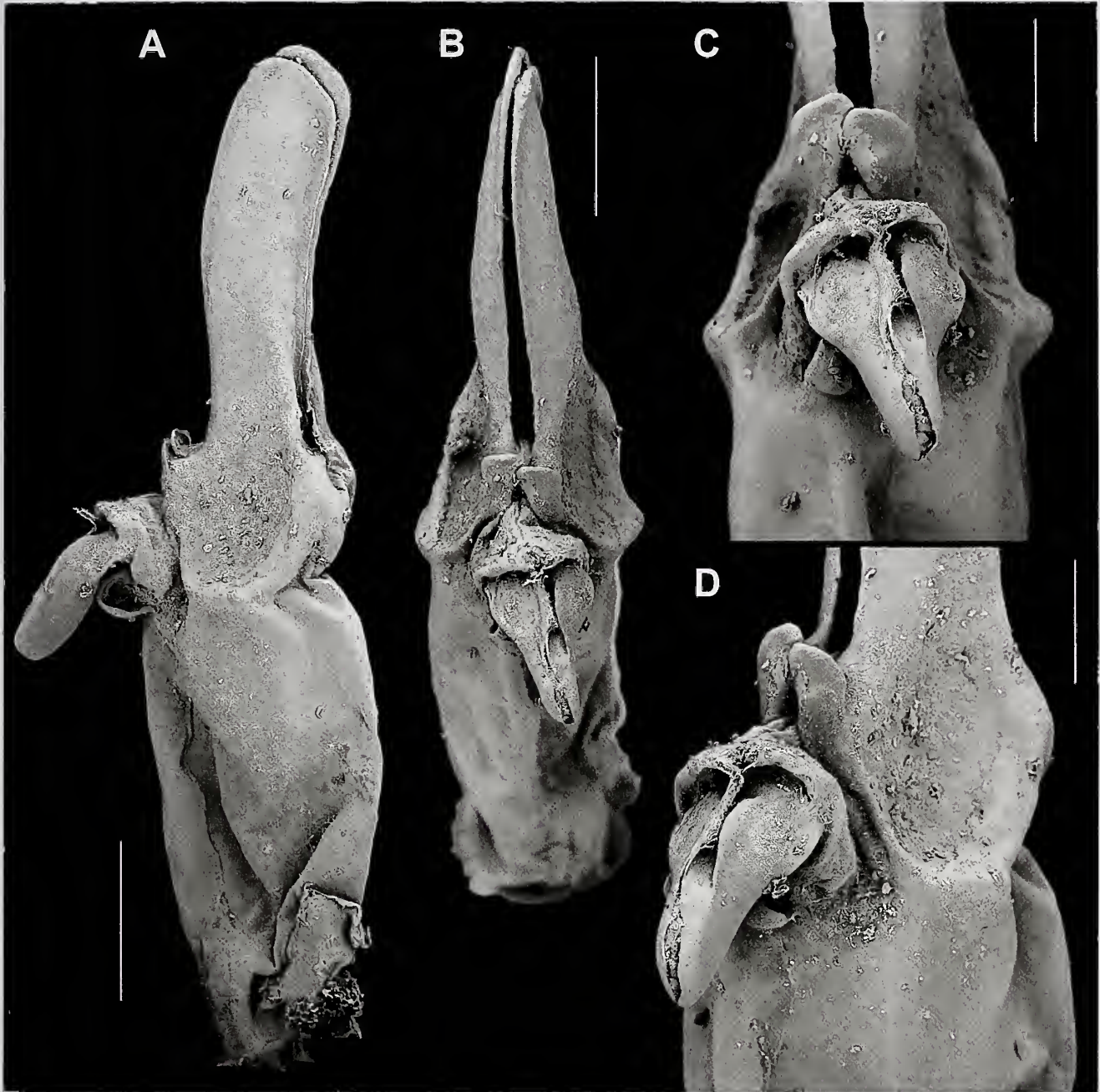


Fig. 25. *Hormiops infulcra* Monod, 2014, male holotype (MHNG, sample VMI-12/14), post-insemination spermatophore. In toto, lateral (A), and upper (B) aspects. Detail of capsular region, anterior aspect (C), rotated approximately 45° counter-clockwise from lateral aspect (D). Scales, 0.5 mm (A-B), 0.25 (C-D).

compared to body size, but also in allometric slopes (Fig. 13B; *H₀*: slopes are equal, likelihood ratio statistic: 6.735, P-value = 0.0094564). Pedipalps are positively allometric in males (slope = 1.33089; lower limit = 1.129663, upper limit = 1.567963; *H₀*: slope not different from 1, test statistic: $r = 0.6046$, P-value = 0.0013684), whereas in females they are isometric (slope = 0.9915464, lower limit = 0.8520906, upper limit = 1.1538258; *H₀*: slope not different from 1, test statistic: $r = -0.02406$, P-value = 0.90911).

Intraspecific variation: Large males have proportionally longer pedipalps than small males as indicated by the positive allometry (Fig. 13B). Pectinal teeth count varies from 5 to 7 in males ($n = 25$, mode = 6), and from 5 to 6 in females ($n = 25$, mode = 5).

Distribution and ecology: *Hormiops infulcra* is only known from two islands of the Seribuat Archipelago (Rompin District, Pahang State, Peninsular Malaysia) and is probably endemic to this group of granitic islands

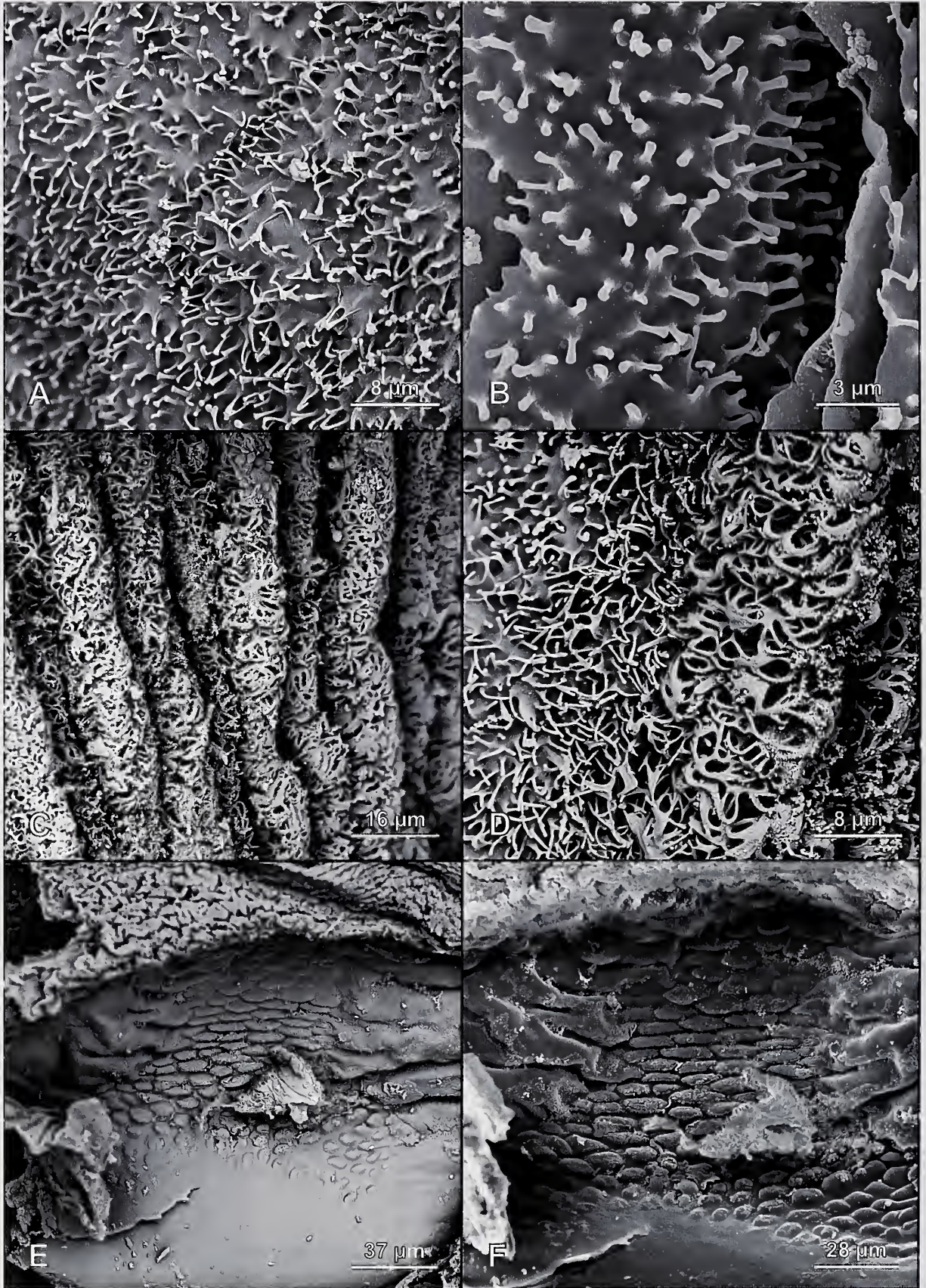


Fig. 26. *Hormiops infulcra* Monod, 2014, book lungs of male paratype (MHNG, sample VMI-12/14). (A-B) Surface of book lung lamella with simple trabeculae. (C-D) Arcuate distal edges of book lung lamellae, posterior view. (D-E) Movable posterior edge of spiracle with hillock-like and chisel-like structures (circle), anterior view.

(Fig. 27). On Pulau Tioman, scorpions were collected in primary rainforests, most of them in narrow crevices of granitic outcrops (Fig. 28). Although these scorpions are primarily stenotopic rock dwellers, a few specimens were found under the bark and in holes of fallen logs or standing trees. It is probable that these were seeking shelter on alternative substrate due to the high population densities of *H. infulcra* on Pulau Tioman and the limited quantity of crevices in granite. *Hormiops infulcra* was found in syntopy (*sensu* Rivas, 1964) with *L. australasiae*. Both species occupy the same microhabitats, i.e. rock crevices and tree holes, however *L. australasiae* was rarely found on rock but was more prevalent on trees. The habitat and habitus of *H. infulcra* are consistent with the lithophilous ecomorphotype (Prendini, 2000).

Conservation status: Most known populations of *H. infulcra* occur in protected rainforests of the Pulau Tioman Wildlife Reserve. The species can be categorized as a short-range endemic because the land area of the islands on which it is found represents about 133.6 km². Although *H. infulcra* is currently not threatened, its restricted distribution range makes the species particularly vulnerable to potential threats from tourism and loss of habitat in the future, and it is

recommended that it be placed in the IUCN Red List of near threatened species (International Union for the Conservation of Nature, 2001).

ACKNOWLEDGEMENTS

Field work in Malaysia and Vietnam was funded in part by the MHNG. The author wishes to express his gratitude to the following persons: (1) Jacqueline Heurtault, Wilson Lourenço and Christine Rollard (MNHN), Lua Hui Keng, Peter Ng and Chang Man Wang (LKCM) for granting access to the collections in their care and preparing loans; (2) Dinh Sac Pham for help with the administrative procedure of getting collecting permits; (3) Matthias Burger, Raphael Covain, Lorenzo Prendini and Peter Schwendinger for providing helpful scientific advice, information and comments, and/or support; (4) Vladimir Timokhanov for producing the habitus colour illustrations; (5) André Piuz for technical assistance with SEM; (6) Camilo Mattoni, Peter Schwendinger and Erieh Volschenk for providing comments on an early draft of the manuscript; (7) Delphine Gaillard and Gwendolyn Romand for assistance during fieldwork.

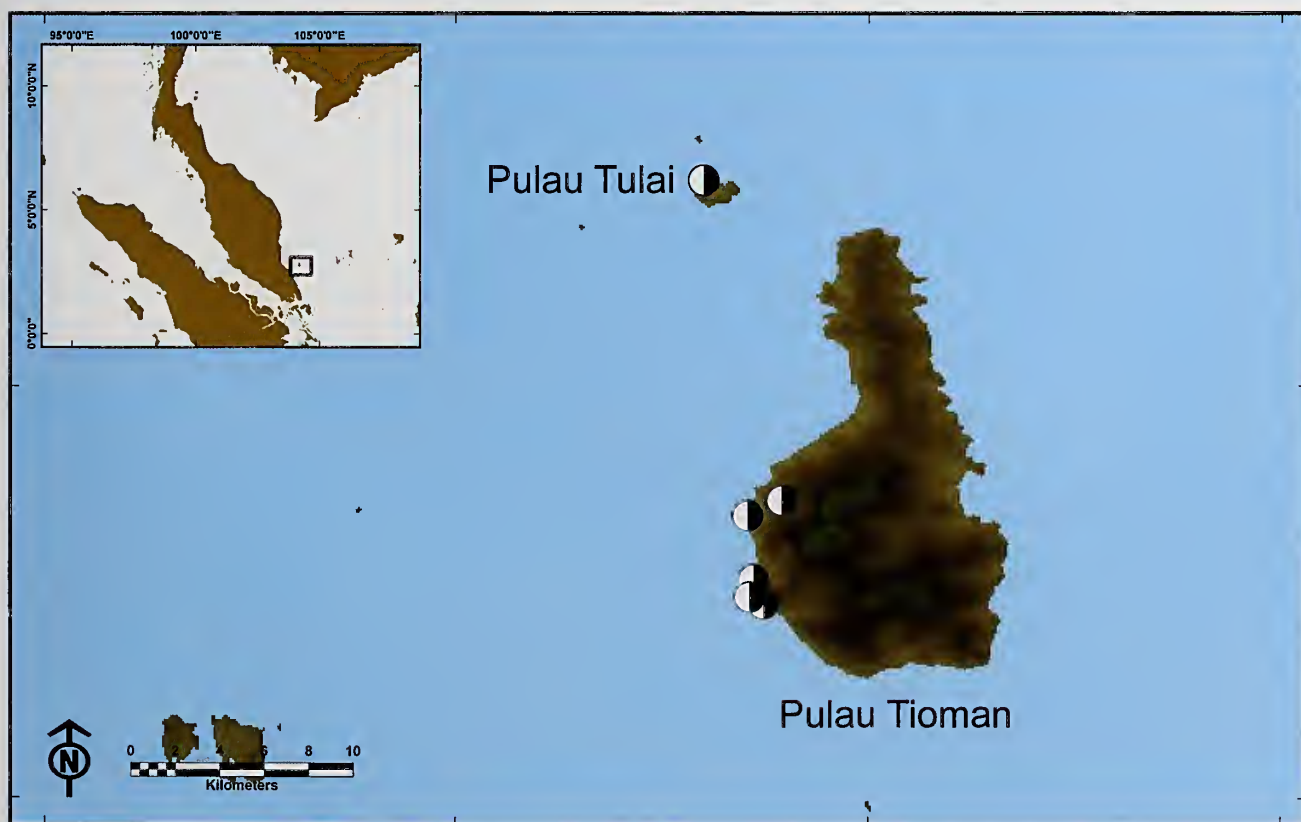


Fig. 27. Known localities of *Hormiops infulcra* Monod, 2014 in the Seribu Archipelago, Pahang, Malaysia, with topography indicated.



Fig. 28. Two biotopes of *Hormiops infulcra* Monod, 2014 on Pulau Tioman, Seribu Archipelago, Pahang, Malaysia.

REFERENCES

- Becker J.J., Sandwell D.T., Smith W.H.F., Braud J., Binder B., Depner J., Fabre D., Factor J., Ingalls S., Kim S.-H., Ladner R., Marks K., Nelson S., Pharaoh A., Trimmer R., Von Rosenberg J., Wallace G., Weatherall P. 2009. Global bathymetry and elevation data at 30 arc seconds resolution: SRTM30_PLUS. *Marine Geodesy* 32: 355-371. Available at http://topex.ucsd.edu/WWW_html/srtm30_plus.html (accessed 2014).
- Bonduriansky R. 2007. Sexual selection and allometry: a critical reappraisal of the evidence and ideas. *Evolution* 61(4): 838-849.
- Chapman A.D., Grafton O. 2008. Guide to best practices for generalising primary species-occurrence data, version 1.0. *Global Biodiversity Information Facility, Copenhagen*, 27 pp. Available at <http://www2.gbif.org/BP sensitivedata.pdf> (accessed 2011).
- Claude J. 2008. Morphometrics with R. *Springer Science/Business Media, New York*, 316 pp.
- Couzijn H.W.C. 1976. Functional anatomy of the walking-legs of Scorpionida with remarks on terminology and homologization of leg segments. *Netherlands Journal of Zoology* 26: 453-501.
- Fabricius J.C. 1775. Entomologia systematica emendata et aucta. Secundum classes, ordines, genera, species, adjectis synonymis, locis, observationibus, descriptionibus. Tomus II. *Hafniae, Impensis Christ. Gottl. Proft*, 519 pp.
- Fage L. 1933. Les scorpions de l'Indochine française, leur affinités, leur distribution géographique. *Annales de la Société Entomologique de France* 102: 25-34.
- Fage L. 1936. Nouvelle contribution à l'étude des scorpions de l'Indochine française. *Bulletin de la Société d'Entomologie de France* 41: 179-181.
- Fage L. 1946. Scorpions et pédipalpes de l'Indochine française. *Annales de la Société entomologique de France* 113: 71-81.
- Fet V. 2000. Family Ischnuridae Simon, 1879 (pp. 383-408). In: Fet V., Sissom W.D., Lowe G., Braunwalder M.E. (eds). Catalog of the scorpions of the world (1758-1998). *NY Entomological Society, New York*, 690 pp.
- Flury B.N. 1984. Common principal components in k groups. *Journal of the American Statistical Association* 79: 892-898.
- Green A.J. 1992. Positive allometry is likely with mate choice, competitive display and other functions. *Animal Behaviour* 43(1): 170-172.
- Harvey M.S. 2002. Short-range endemism in the Australian fauna: some examples from non-marine environments. *Invertebrate Systematics* 16: 555-570.
- International Union for the Conservation of Nature (IUCN) 2001. IUCN Red List categories and criteria. Version 3.1. *IUCN Species Survival Commission, IUCN, Gland/Cambridge*. Available from http://www.iucnredlist.org/static/categories_criteria (accessed 2014).
- Jarvis A., Reuter H.I., Nelson A., Guevara E. 2008. Hole-filled seamless SRTM data V4. *International Centre for Tropical Agriculture (CIAT)*. Available at <http://srtm.csi.cgiar.org> (accessed 2014).
- Kamenz C., Dunlop J.A., Scholtz G. 2005. Characters in the book lungs of Scorpiones (Chelicerata, Arachnida) revealed by scanning electron microscopy. *Zoomorphology* 124: 101-109.
- Kamenz C., Prendini L. 2008. An atlas of book lung fine structure in the order Scorpiones (Arachnida). *Bulletin of the American Museum of Natural History* 316: 1-45.
- Kästner A. 1941. 1. Ordnung der Arachnida: Scorpiones (pp. 229-240). In: Kükenthal W., Krumbach T. (eds). *Handbuch der Zoologie, Band 3, Häfte 2, Teil 1. Walter de Gruyter Verlag, Berlin*.
- Kermack K.A., Haldane J.B.S. 1950. Organic correlation and allometry. *Biometrika* 37: 30-41.
- Kovářík F. 1998. Štíři (Scorpions). *Nakladatelski Madagaskar, Jihlava*, 175 pp.
- Kovářík F. 2000. First record of *Liocheles nigripes* from Indonesia and Malaysia and *Hormiops davidovi* from Malaysia (Scorpiones: Ischnuridae). *Acta Societatis Zoologicae Bohemoslovacae* 64: 57-64.
- Kovářík F. 2005. Two new species of the genus *Chaerilus* Simon, 1877 from Malaysia (Scorpiones: Chaerilidae). *Euscorpius* 26: 1-9.
- Kovářík F. 2012a. *Euscorpiops thaomischii* sp. n. from Vietnam and a key to species of the genus (Scorpiones: Euscorpiidae: Scorpiopinae). *Euscorpius* 142: 1-10.
- Kovářík F. 2012b. Five new species of *Chaerilus* Simon, 1877 from China, Indonesia, Malaysia, Philippines, Thailand, and Vietnam (Scorpiones: Chaerilidae). *Euscorpius* 149: 1-14.
- Kovářík F. 2013. *Alloscorpiops wrongpromi* sp. n. from Thailand and Laos (Scorpiones: Euscorpiidae: Scorpiopinae). *Euscorpius* 160: 1-14.
- Lamoral B.H. 1979. The scorpions of Namibia (Arachnida: Scorpionida). *Annals of the Natal Museum* 23(3): 497-784.
- Lourenço W.R. 1989. Rétablissement de la famille des Ischnuridae, distincte des Scorpionidae Pocock, 1893, à partir de la sous-famille des Ischnurinae Pocock, 1893. *Revue Arachnologique* 8(10): 159-177.
- Lourenço W.R. 2011. Scorpions from the Island of Côn Sơn (Poulo Condore), Vietnam and description of a new species of *Chaerilus* Simon, 1877 (Scorpiones, Chaerilidae). *Comptes Rendus Biologies* 334: 773-776.
- Lourenço W.R. 2013. A new species of *Euscorpiops* Vachon, 1980 from Laos (Scorpiones: Euscorpiidae: Scorpiopinae). *Acta Arachnologica* 62(1): 23-27.
- Lourenço W.R., Monod L. 1999. Confirmation de la validité du genre *Hormiops* Fage, 1933 avec redescription d'*Hormiops davidovi* Fage, 1933 (Scorpiones, Ischnuridae). *Zoosystema* 21(2): 337-344.
- Lourenço W.R., Pham D.S. 2013. First record of a cave species of *Euscorpiops* Vachon from Viet Nam (Scorpiones, Euscorpiidae, Scorpiopinae). *Compte Rendus Biologies* 336(7): 370-374.
- Mirza Z.A., Sanap R.V., Upadhye R. 2014. A new species of scorpion of the genus *Neoscorpiops* Vachon, 1980 (Scorpiones: Euscorpiidae) from India. *Comptes Rendus Biologies* 337(2): 143-149.
- Monod L. 2011. Taxonomic emendations in the genus *Liocheles* Sundevall, 1833 (Scorpiones, Liochelidae). *Revue suisse de Zoologie* 118(4): 723-758.
- Monod L. 2014. The genus *Hormiops* Fage, 1933 (Hormuridae, Scorpiones), a palaeoendemic of the South-China Sea: systematics and biogeography. *Comptes Rendus Biologies* 337: 596-608.
- Monod L., Harvey M.S., Prendini L. (2013). Stenotopic *Hormurus* Thorell, 1876 scorpions from the monsoon ecosystems of northern Australia, with a discussion on the evolution of burrowing behaviour in Hormuridae Laurie, 1896. *Revue suisse de Zoologie* 120(2): 281-346.

- Monod L., Prendini L. 2015. Evidence for Eurogondwana: The roles of dispersal, extinction and vicariance in the evolution and biogeography of Indo-Pacific Hormuridae (Scorpiones: Scorpionoidea). *Cladistics* 31: 71-111.
- Monod L., Volschenk E.S. 2004. *Liocheles litodactylus* (Scorpiones: Liochelidae): an unusual new *Liocheles* species from the Australian Wet Tropics (Queensland). *Memoirs of the Queensland Museum* 49(2): 675-690.
- Prendini L. 2000. Phylogeny and classification of the superfamily Scorpionoidea Latreille, 1802 (Chelicerata, Scorpiones): an exemplar approach. *Cladistics* 16: 1-78.
- Prendini L. 2001. Substratum specialization and speciation in southern African scorpions: the Effect Hypothesis revisited (pp. 113-138). In: Fet V., Selden P.A. (eds). *Scorpions 2001. In memoriam Gary A. Polis. British Arachnological Society, Burnham Beeches, Bucks*, 404 pp.
- R Development Core Team 2011. R: A language and environment for statistical computing. *R Foundation for Statistical Computing, Vienna, Austria (ISBN 3-900051-07-0)*. Available from <http://www.R-project.org> (accessed 2014).
- Ricker W.E. 1984. Computation and uses of central trend lines. *Canadian Journal of Zoology* 62(10): 1897-1905.
- Rivas L.R. 1964. A reinterpretation of the concepts "sympatric" and "allopatric" with proposal of the additional terms "syntopic" and "allotopic". *Systematic Biology* 13: 42-43.
- Stahnke H.L. 1970. Scorpion nomenclature and mensuration. *Entomological News* 81: 297-316.
- Stahnke H.L. 1972. UV light, a useful field tool. *Bioscience* 22: 604-607.
- Sundevall C.J. 1833. *Conspectus Arachnidum. Sveno Hardin et Erico T. Hammergren, Vermlandis, London-Göteborg*, 39 pp.
- Takashima H. 1945. Scorpions of Eastern Asia. *Acta Arachnologica* 9(3-4): 68-106.
- Vachon M. 1956. Sur des nouveaux caractères familiaux et génériques chez les scorpions (pp. 471-474). In: *Proceedings of the XIV International Congress of Zoology, Copenhagen, 5-12 August 1953. Danish Science Press, Copenhagen*, 567 pp.
- Vachon M. 1963. De l'utilité, en systématique, d'une nomenclature des dents des chélicères chez les scorpions. *Bulletin du Muséum National d'Histoire Naturelle (Serie 2)* 35: 161-166.
- Vachon M. 1974. Etude des caractères utilisés pour classer les familles et les genres de scorpions (Arachnides). 1. La trichobothriotaxie chez les scorpions. *Bulletin du Muséum National d'Histoire Naturelle (Serie 3)* 140: 857-958.
- Volschenk E.S. 2002. Systematic revision of the scorpion genera in the family Buthidae. *Ph.D. thesis, Curtin University of Technology*, 224 pp.
- Volschenk E.S. 2005. A new technique for examining surface morphosculture of scorpions. *Journal of Arachnology* 33: 820-825.
- Warton D.I., Weber N. C. 2002. Common slope tests for errors-in-variables models. *Biometrical Journal* 44: 161-174.
- Warton D.I., Duursma R., Falster D., Taskinen S. 2011. Package SMATR version 3.2.3. Available from "<http://cran.r-project.org/>" (accessed 2014).
- Warton D.I., Duursma R., Falster D.S., Taskinen S. 2012. SMATR 3 - an R package for estimation and inference about allometric lines. *Methods in Ecology and Evolution* 3: 257-259.
- Warton D.I., Wright I.J., Falster D.S., Westoby M. 2006. Bivariate line-fitting methods for allometry. *Biological Reviews* 81(2): 259-291.